Decreased Expression of Synaptophysin 1 (SYP1 Major Synaptic Vesicle Protein p38) and Contactin 6 (CNTN6/NB3) in the Cerebellar Vermis of reln Haplodeficient Mice

Decreased expression of synaptophysin 1 (SYP1 major synaptic vesicle protein p38) and contactin 6 (CNTN6/NB3) in the cerebellar vermis of *reln* haplodeficient mice

Claudia Castagna, Adalberto Merighi, Laura Lossi

University of Turin, Department of Veterinary Sciences, Turin, Italy

Correspondence to Claudia Castagna

Department of Veterinary Sciences, Largo Paolo Braccini 2, I-10095 Grugliasco (TO) Italy; phone: +390116709128; e-mail: claudia.castagna@unito.it

Claudia Castagna ORCID 0000-0003-1097-7547, Adalberto Merighi ORCID 0000-0002-1140-3556, Laura Lossi ORCID 0000-0003-1149-212X

Abstract

Reeler heterozygous mice (*reln*$^{+/-}$) are seemingly normal but haplodeficient in *reln*, a gene implicated in autism. Structural/neurochemical alterations in the *reln*$^{+/-}$ brain are subtle and difficult to demonstrate. Therefore, the usefulness of these mice in translational research is still debated. As evidence implicated several synapse-related genes in autism and the cerebellar vermis is structurally altered in the condition, we have investigated the expression of synaptophysin 1 (SYP1) and contactin 6 (CNTN6) within the vermis of *reln*$^{+/-}$ mice.

Semi-thin plastic sections of the vermis from adult mice of both sexes and different genotypes (*reln*$^{+/-}$ and *reln*$^{+/+}$) were processed with an indirect immunofluorescence protocol. Immunofluorescence was quantified on binary images and statistically analyzed.

Reln$^{+/-}$ males displayed a statistically significant reduction of 11.89% in the expression of SYP1 compared to sex-matched wild-type animals, whereas no differences were observed between *reln*$^{+/+}$ and *reln*$^{+/-}$ females. In *reln*$^{+/-}$ male mice, reductions were particularly evident in the molecular layer: 10.23% less SYP1 than *reln*$^{+/+}$ males and 5.84% less than *reln*$^{+/+}$ females. In *reln*$^{+/-}$ females, decrease was 9.84% *vs* *reln*$^{+/+}$ males and 5.43% *vs* *reln*$^{+/+}$ females. Both *reln*$^{+/-}$ males and females showed a stronger decrease in CNTN6 expression throughout all the three cortical layers of the vermis: 17-23% in the granular layer, 24-26% in the Purkinje cell layer, and 9-14% in the molecular layer. Altogether, decrease of vermian SYP1 and CNTN6 in *reln*$^{+/-}$ mice displayed patterns compatible with the structural modifications of the autistic cerebellum. Therefore, these mice may be a good model in translational studies.

Keywords
Reelin, Cerebellum, Heterozygous, Synaptophysin 1, Contactin 6, Vermis, Synapses

Introduction

Several studies have linked autism with deficits in synaptic structure and function, and synaptic alterations in several brain areas were suggested to contribute to the physiopathology of the autistic syndrome. There is a long list of "synaptic genes" whose mutation predisposes to autism, among which are *BCKDK, CNTN6, CNTNAP2, PTEN, RELN, SHANK3, SYN1 and SYNGAP1* (see Keller et al. 2017 for review, Mercati et al. 2017). These genes encode for proteins that intervene in important biochemical pathways within the cell, such as *BCKDK* and *PTEN*; have a role in cell-to-cell interactions, such as *CNTNAP2*, CNTN6, *RELN* and *SYNGAP1*; or are directly expressed at synapses, as it is the case for *SHANK3* and *SYN1*. Yet, structural modifications of synapses in the autistic brain are subtle: they were reported both pre- and post-synaptically and affected, at different degrees, the synapses in various brain areas that are primarily linked with the autistic pathologic phenotype such as *e.g.* the prefrontal cortex and hippocampus.

Among the better characterized marker proteins of the synaptic vesicles are the synaptophysins (SYPs - Thiel 1993). There are at least two SYPs in brain, SYP1 (Navone et al. 1986) and SYP2, the latter being also referred to as synaptoporin. The two SYPs display similar properties, are present on the same synaptic vesicles, but do not co-assemble (Fykse et al. 1993). SYP1 is approximately 6% of the total synaptic vesicle protein content and is homogeneously expressed in central synapses, whereas SYP2 is only detected in synapses made by selected neuronal populations (Fykse et al. 1993). For its abundance, studies on the autistic brain have obviously been focused onto SYP1. Being autism a neurodevelopmental disorder with well-defined behavioral alterations, an interest for SYP1 in relation to the autistic pathology was raised after the observation that the protein regulated the activity-dependent formation of synapses in cultured hippocampal neurons (Tarsa and Goda 2002) and that mice lacking SYP1 displayed behavioral alterations and learning deficits resembling those observed in autism (Schmitt et al. 2009). In keeping with these observations, Western blot analysis on postnatal mice treated with an agonist of the vasoactive intestinal peptide receptor 2, which is expressed at higher levels in the lymphocytes of autistic patients, revealed significant reductions of SYP1 in the prefrontal cortex, but not in the hippocampus (Ago et al. 2015). Conversely, rats treated with valproic acid to experimentally model autism, showed an upregulation of SYP1 in cultured primary neural progenitor cells (Kim et al. 2017) and increased SYP1 immunostaining in the prefrontal cortex, but a decrease of protein levels in all hippocampal subfields (Codagnone et al. 2015). Therefore, although, these studies support the notion that SYP1 may be involved in the structural alterations of the autistic synapses, they are not conclusive about the possibility that modifications in SYP1 levels may be different in the different areas of the brain that may be hit by the autistic pathology.

Although developmental abnormalities and early injury in cerebellum have been implicated in the development of autism, there is an array of opinions as regarding the involvement of a synaptic pathology in the condition (Fatemi et al. 2012). Such a debate has been generated primarily because the molecular mechanisms underlying the loss of the cerebellar Purkinje neurons reported in certain studies on autistic patients are still unclear (see below).

However, very recently, observations on these cerebellar neurons, which were derived from human induced pluripotent stem cells obtained from patients with a pathogenic tuberous sclerosis complex 2 mutation - a disorder often coexisting with autism - reported a decreased expression of SYP1, give further support to the possibility that the protein is somewhat implicated in the autistic pathology also in cerebellum (Sundberg et al. 2018).

The mammalian cerebellum is very compact, and, in humans, it harbors about 80% of the brain neurons, but equals to only about 10% of the brain volume; on the opposite, the cerebral hemispheres (cortex + white matter) contain only 19% of the brain neurons but represent about 82% of the brain mass (Azevedo et al. 2009). From these numbers it obviously appears that compactness makes an accurate structural and functional investigation of the cerebellum a quite difficult task to perform (Schlerf et al. 2015).

The percentages reported above for humans are somewhat maintained throughout mammals, so that, on average, a ratio of 3.6 neurons in the cerebellum to every neuron in the cerebral cortex occurs across species, with figures of about 2.6 and 4.1 for primates and rodents, respectively (Herculano-Houzel 2010). Analogies between the cerebellar and the cerebral cortices are numerous, but on the top of them stays their layered structure that is consequent to a very peculiar developmental modality (McConnell 1995).Therefore, it is not unexpected that both express high levels of reelin, a large glycoprotein of the extracellular matrix playing a fundamental role in neuronal migration and correct positioning (Andersen et al. 2002; Tissir and Goffinet 2003).

The protein was so named after the discovery of its coding gene, and the recognition that its absence was causative of a spontaneous mutation called *Reeler* (D'Arcangelo et al. 1995), which was described several decades before as being characterized by an ataxic walk of the affected mice (Falconer 1951). The mutation is autosomic and displays a recessive transmission. Thus, only homozygous recessive *Reeler* mice (*reln*$^{-/-}$) completely lack reelin and have a typical phenotype affecting the cerebellum. Behavioral signs in homozygous mutants are dystonia, ataxia, and tremor; in parallel, there are structural alterations of their nervous system that primarily impact upon the architecture of the cerebral and cerebellar cortices and hippocampus (Caviness and Rakic 1978; Goffinet 1984).

Differently from the recessive mutants, heterozygous *Reeler* mice (*reln*$^{+/-}$) appear phenotypically normal but have attracted the interest of the neurologists as putative translational models for human autism (Fatemi et al. 2012). Soon after the initial discovery in mouse, it was in fact demonstrated that the causative gene was highly conserved between mice (*reln*) and humans (*RELN*) (DeSilva et al. 1997), association studies indicated that *RELN* was linked to the autistic cerebellar pathology (Fatemi 2005; Hong et al. 2000; Lammert and Howell 2016), and Reelin was shown to be down-regulated in the autistic cerebellum after SDS-gel electrophoresis and Western blotting (Fatemi et al. 2001).

Long before these studies, the occurrence of structural alterations in the cerebellum of the autistic patients was well established, as the first post-mortem report on the numerical reduction of the cerebellar Purkinje neurons in these patients was published in the mid-eighties of the last century (Bauman and Kemper 1985). To this initial observation,

numerous other confirmative studies followed also regarding the size of these cells (see Fatemi et al. 2012 for references), as well as the demonstration of additional histological alterations affecting the cerebellar nuclei (Kemper and Bauman 1998). Interestingly, however, the reduction in number and size of vermal Purkinje neurons was not confirmed at subsequent histopathology examinations (Fatemi et al. 2012). This was a somewhat puzzling finding if one considers that hypoplasia of vermian lobules VI and VII was often described in infantile autism following an initial, widely-quoted MRI study (Courchesne et al. 1988), to which another survey followed indeed demonstrating the existence of two subtypes of infantile autism, one with hypoplasia and the other with hyperplasia of the vermis (Courchesne et al. 1994).

It is notable that most of the histological modifications observed in the human autistic cerebellum are similar to those described in the few studies carried on *reln*$^{+/-}$ mice. These studies reported a loss of the GABAergic Purkinje neurons (Maloku et al. 2010; Magliaro et al. 2016) and modifications in the size of these cells, as well as in their alignment along the YZ axis of cerebellum (Magliaro et al. 2016). In addition to structural alterations of their brain, *reln*$^{+/-}$ mice were described to display behavioral features like those in autism or other neuropsychiatric disorders (Tueting et al. 1999; Brigman et al. 2006; Ognibene et al. 2007; Teixeira et al. 2011). However, other investigations failed, partly or in full, to substantiate such analogies (Salinger et al. 2003; Podhorna and Didriksen 2004; Krueger et al. 2006; Michetti et al. 2014). Discrepancies in behavioral data are not surprising as the identification of suitable animal models of autism is challenging. This because autistic behaviors in humans are primarily related to social interaction, communication, and restricted interests, and these behaviors are obviously very difficult to be objectively measured in mice (Bey and Jiang 2014).

To get further insight on the usefulness of the *reln*$^{+/-}$ mouse as a translational model of autism, we report here the results of a quantitative estimation of the levels of expression of SYP1 (major synaptic vesicle protein p38 - Navone et al. 1986) and CNTN6 (Stoeckli 2010), in the cerebellar vermis of normal and *reln* haplodeficient mice of both sexes.

Methods

Animals

Studies were performed on twelve adult mice (> 2 months) of both sexes and different *reln* genetic backgrounds (*reln*$^{+/-}$ and *reln*$^{+/+}$) that were divided in four experimental groups: *reln*$^{+/+}$ males, *reln*$^{+/+}$ females, *reln*$^{+/-}$ males, and *reln*$^{+/-}$ females. The number of animals was kept to a minimum and all efforts were made to minimize their suffering. All experiments were authorized by the Italian Ministry of Health and the Bioethics Committee of the University of Turin. Animal procedures were carried out according to the guidelines and recommendations of the European Union (Directive 2010/63/UE) as implemented by current Italian regulations on animal welfare (DL n. 26-04/03/2014). Before being used in this study, all animals were sexed and genotyped by routine methods to ascertain their *reln* genetic background (D'Arcangelo et al. 1996).

Tissue preparation and sampling strategy

Animals were deeply anesthetized with an overdose of sodium pentobarbital and perfused with 4% paraformaldehyde in 0.1M phosphate buffer (PB), pH 7.4-7.6. Dissected brains were then post-fixed overnight in the same fixing solution. After several washes in PB, the cerebellar vermis was dissected and cryoprotected overnight in 30% sucrose in phosphate buffered saline (PBS). It was then cut with a vibrating microtome (Leica VT1000S, Germany) in 200 µm-thick serial parasagittal slices that were subsequently dehydrated with increasing grade alcohols up to 70% and flat embedded in LR-White resin (Soiza-Reilly 2015). Embedding in LR-White was employed as antibodies cannot penetrate the plastic (Brorson et al. 1994). Therefore the immunoreaction only occurred at the surface of sections and the immunofluorescence signal could be accurately quantified.

Sampling strategy was as follows (Fig. 1A): two randomly-chosen slices were selected from each series cut through the longitudinal axis of the vermis and further cut in 2 µm semi-thin sections with an ultramicrotome (Leica EM UC6). Several series of four sequential semi-thin parasagittal sections encompassing the entire vermis were then collected on glass slides. Of these, two randomly-chosen series, separated by at least 50 µm along the transversal axis of cerebellum, were selected and processed for histology. In each selected series the first three sections were processed for immunocytochemistry, and stained with 4′,6-diamidino-2-phenylindole (DAPI) diluted in PBS at a concentration of 2 µg/ml (Fig. 1B), in order to properly identify individual lobules and define the borders of the three cortical layers. Of the three immunostained sections, one was selected at random and processed further as described below.

Immunofluorescence

LR-White sections were washed 5 min in filtered PBS 0.01 M pH 7.4 and blocked for 5 min in PBS containing 5% normal goat serum (NGS - Sigma Aldrich, MO, USA) and 0.1% Triton X-100 (Sigma Aldrich). Sections were then put in a humid chamber and incubated for two hours at room temperature in the rabbit primary antibodies against SYP1 [#batch 32a (G95) a kind gift from Dr R. Jahn, Max-Plank-Institut fuer Psychiatrie] or contactin 6 (CNTN6 - Antibodies-online ABIN 350255), a marker - among others - of the mature granule cells and the synapses made by the parallel fibers (Stoeckli 2010). Primary antibodies were diluted 1:200 (SYP1) or 1:400 (CNTN6) in a diluent made of 0.2% poly-L-lysine, 0.2% bovine serum albumin (BSA) in PBS. After being rinsed 3x5 min in filtered PBS, sections were incubated for 1 hour with the anti-rabbit Alexa Fluor® 594 fluorescent antibody conjugate (Molecular Probes, Life Technology, USA) diluted 1:200 in the same diluent used for the primary antibody. After three gentle washes in filtered PBS, slides were mounted in a preserving fluorescence medium (Fluoroshield, Sigma Aldrich).

Immunostained sections were observed at a 63x magnification with a wide-field fluorescence light microscope (DM6000B, Leica, Germany). Randomly selected images (1392x1040 pixel, pixel size: 6.823x6.823 µm) of the cerebellar cortex were acquired with a digital camera and, for SYP1, analyzed as resumed in Fig. 1. Quantitative analysis of CNTN6 was performed using the same approach but on a reduced number of sections

(30/genotype) and was limited to whole vermis and the separate cortical layers, without considering singly the lobules. Image acquisition conditions were maintained unaltered throughout all the different batches of experiments.

ImageJ processing

Images were loaded with ImageJ and converted to binary (background=0; fluorescence signal=1 – Fig. 1D) by the ImageJ software (http://imagej.nih.gov/ij/). Using the DAPI-stained sections as a reference, the operator sequentially defined three regions of interest (ROIs) corresponding to the molecular layer, the Purkinje cells' layer and the granular layer of the cerebellar cortex. Then, the command «analyze particles» was launched to automatically extract the percentage of the fluorescent area (PFA) *vs* the total area of the section. Raw data were stored in a Microsoft Excel spreadsheet for subsequent statistical analysis (Online Resource OR1 and OR3).

Statistics

Sample sizes were estimated in advance based on a similar, previously conducted study (Magliaro et al. 2016). No statistical methods were used to predetermine sample size, but a *post-hoc* analysis was carried out using G*Power Version 3.19.2 (http://www.gpower.hhu.de/). Every step used to process and analyze data was planned in advance as a part of the experimental protocol (Fig. 1). Statistical analyses were performed using GraphPadPrism®7 (GraphPadSoftware, CA, USA) or the Excel add-in Realstats-2010 (http://www.real-statistics.com/).

Outliers were identified with GraphPadPrism®7 after ROUT (Q = 0.1%). The same software was employed to apply D'Agostino & Pearson omnibus normality test to check for normally distributed data. Comparisons between two groups (males *vs* females or *reln*$^{+/+}$ *vs reln*$^{+/-}$) were made using the unpaired two-tailed Mann-Whitney test. Multiple comparisons were made using ordinary one-way ANOVA for normally distributed data followed by Tukey's multiple comparisons test, or the non-parametric Kruskal-Wallis test followed by Dunn's multiple comparisons test. To analyze the effect of the interaction between two different factors (*reln* genotype and sex or genotype and cerebellar lobule) the Scheirer Ray Hare test, the two factor version of the Kruskal-Wallis test, was employed. Data are reported as means±95% confidence interval (CI). Differences were considered statistically significant for $P<0.01$.

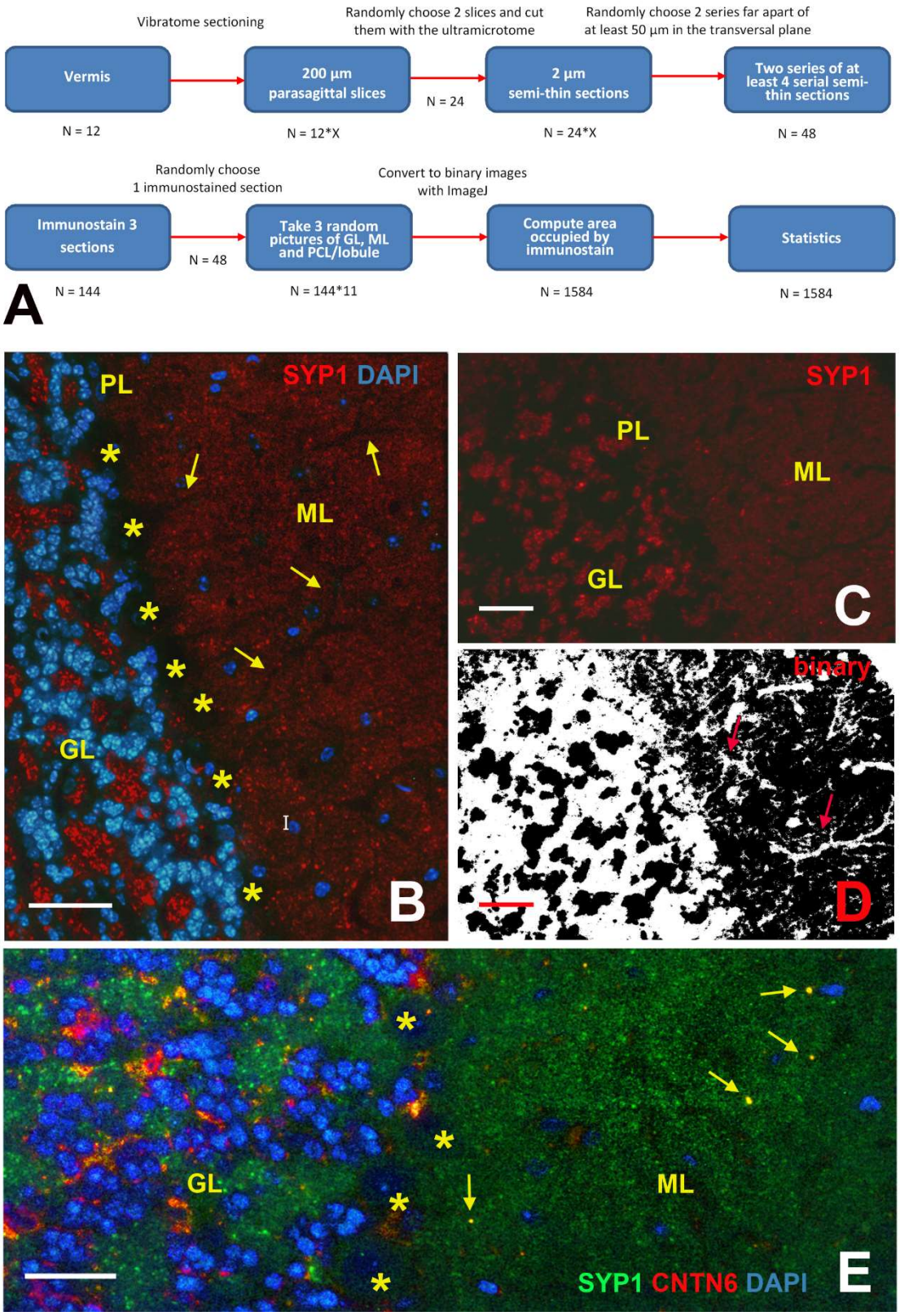

Fig. 1 Method for quantitative analysis of SYP1 immunostaining

A: Statistics' plan; **B-D** recognition of cortical layers in immunostained sections. Image in **B** is exemplificative of the appearance of the cerebellar cortex after SYP1 (red) and DAPI (blue) dual labeling. The synaptophysin-immunostained image in **C** is shown in **D** after it was made binary with the ImageJ software. **E**: double immunostaining for SYP1 (green) and CNTN6 (red) in a *reln+/+* male. Note the colocalization (yellow) of the two labels in the granular layer's glomeruli and in the molecular layer. Note also the CNTN6+ cell bodies of

some Golgi cells in the granular layer. The asterisks in **B** and **E** indicate the areas occupied by the cell bodies of the Purkinje neurons that are aligned to form the PL. The arrows in **B** and **D** indicate some of the main trunks and branches forming the Purkinje neurons' dendritic arborizations. The arrows in **E** show the puncta of colocalization (yellow) between SYP1 and CNTN6. *Abbreviations*: CNTN6 = contactin 6; GL = granular layer of cerebellar cortex; ML = molecular layer of cerebellar cortex; PL = Purkinje cells' layer of cerebellar cortex; SYP1 = synaptophysin 1. Scale bars = 50 μm.

Results

Immunocytochemical distribution of SYP1 and CNTN6

The immunocytochemical distribution of SYP1 and CNTN6 in the cerebellar vermis of different *reln* genetic backgrounds is shown in Fig. 1B-C, E, 2 and 3. SYP1 immunoreactivity (Fig. 1B-C, 2) took the form of a very fine punctate reaction in the molecular layer and a much coarser reaction in the granular layer, where the denser patches of SYP1 immunoreactivity very precisely depicted the cerebellar glomeruli intermingled with clusters of granule cells (Fig. 1B). The Purkinje cell layer was, instead, identified by the presence of the large-sized negative cell bodies of the Purkinje neurons that were well aligned at the interface between the other two layers of the cerebellar cortex (Fig. 1B). There were no obvious differences in this pattern of distribution among genotypes (Fig. 2). Quantitative differences were very subtle and cannot be spotted easily by the simple inspection of individual micrographs.

Consistently with the literature (Stoeckli 2010), in normal *reln*$^{+/+}$ mice CNTN6 (Fig. 1E, 3A) was expressed in the molecular layer and the granular layer. CNTN6 immunoreactive puncta were scattered in the former, some also being stained for SYP1 in double immunofluorescence labeling (Fig. 1E). In the granular layer, the cell bodies of the Golgi cells were immunoreactive as well as the cerebellar glomeruli (Fig. 1E, 3A). The latter often displayed colocalization of CNTN6 and SYP1 (Fig. 1E). Again, there are no obvious differences in this pattern of distribution among genotypes (Fig. 3).

Quantitative analysis of SYP1 immunofluorescence

Before comparing the four experimental groups of this study we have verified the absence of statistically significant differences between animals of the same genotype (Online Resource OR2). We have then investigated SYP1 immunoreactivity in the whole vermis, single cortical layers, and individual lobules in different genotypes. For simplicity, results are resumed in graphic form in Table 1.

Whole vermis

Males vs females

When the cerebellar vermis of males and females were compared irrespectively of the *reln* genotype, the means of PFA were not statistically different in the two groups (mean ± CI: males = 71.35 ±1.14; females: 72.53 ± 1.12; two-tailed Mann-Whitney test P =0.0971).

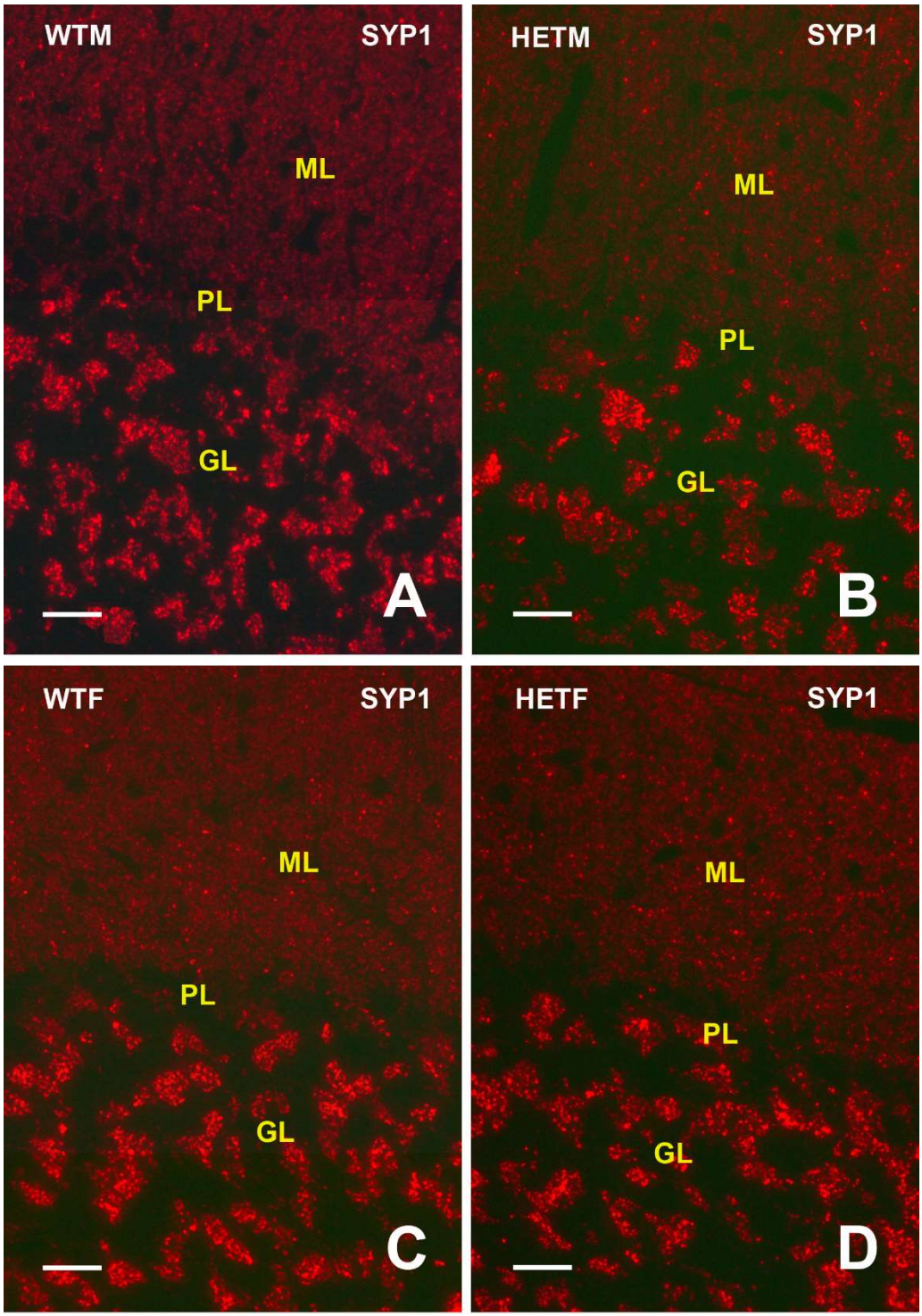

Fig. 2 Expression of SYP1 in different mouse reln genotypes

Exemplificative images of the pattern of distribution of SYP1 in the cerebellar cortex in *reln*$^{+/+}$ males (**A**), *reln*$^{+/-}$ males (**B**), *reln*$^{+/+}$ females (**C**), and *reln*$^{+/-}$ females (**D**). Note that there are no obvious difference in the pattern and intensity of immunostaining, although staining in the molecular layer of *reln*$^{+/-}$ males (**B**) appears slightly less intense.

Abbreviations: GL = granular layer of cerebellar cortex; HETF = *reln*$^{+/-}$ *fe*males; HETM = *reln*$^{+/-}$ males; ML = molecular layer of cerebellar cortex; PL = Purkinje cells' layer of cerebellar cortex; SYP1 = synaptophysin 1; WTF = *reln*$^{+/+}$ females; WTM = *reln*$^{+/+}$ males. Scale bars = 50 μm.

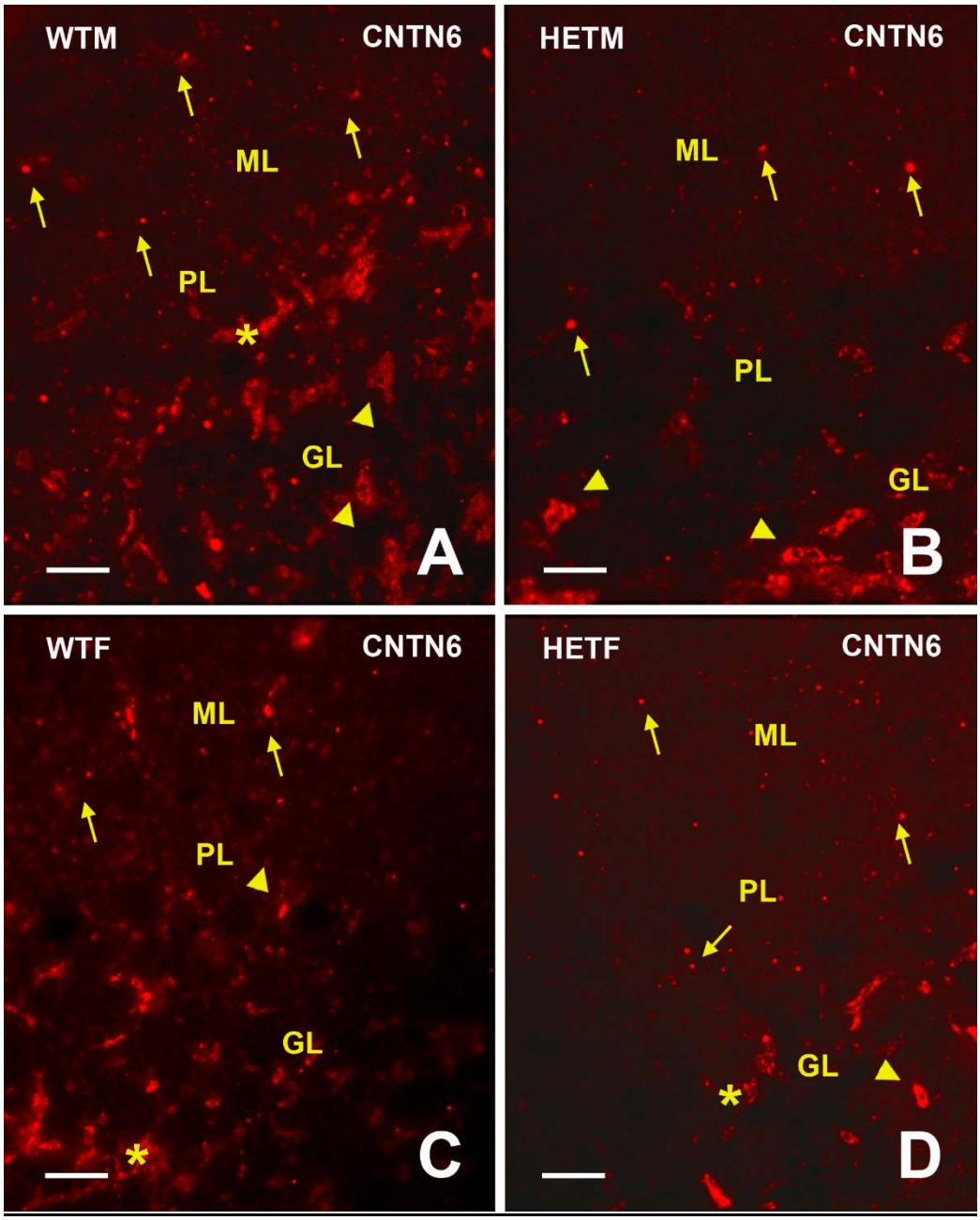

Fig. 3 Expression of CNTN6 in different mouse reln genotypes
Exemplificative images of the pattern of distribution of CNTN6 in the cerebellar cortex in *reln*$^{+/+}$ males (**A**), *reln*$^{+/-}$ males (**B**), *reln*$^{+/+}$ females (**C**), and *reln*$^{+/-}$ females (**D**). Note that there are no obvious difference in the pattern and intensity of immunostaining. The arrows indicate immunoreactive puncta in the molecular layer, the arrow-heads the immunostained Golgi cells, the asterisks the glomeruli.
Abbreviations: GL = granular layer of cerebellar cortex; HETF = *reln*$^{+/-}$ *f*emales; HETM = *reln*$^{+/-}$ males; ML = molecular layer of cerebellar cortex; PL = Purkinje cells' layer of cerebellar cortex; WTF = *reln*$^{+/+}$ females; WTM = *reln*$^{+/+}$ males. Scale bars = 50 μm.

Wild-type vs heterozygous mice

Fig. 4A shows the exploratory data analysis of the vermis of wild-type and heterozygous mice. When wild-type and heterozygous *reln*$^{+/-}$ mice were compared irrespectively of sex (Fig. 4B), the two groups were statistically different (mean ± CI: wild-type = 74.80 ± 1.11;

reln$^{+/-}$: 69.08 ± 1.11; two-tailed Mann-Whitney test P<0.0001). Specifically, *reln*$^{+/-}$ mice displayed a reduction of 7.65% in PFA compared to wild-type mice.

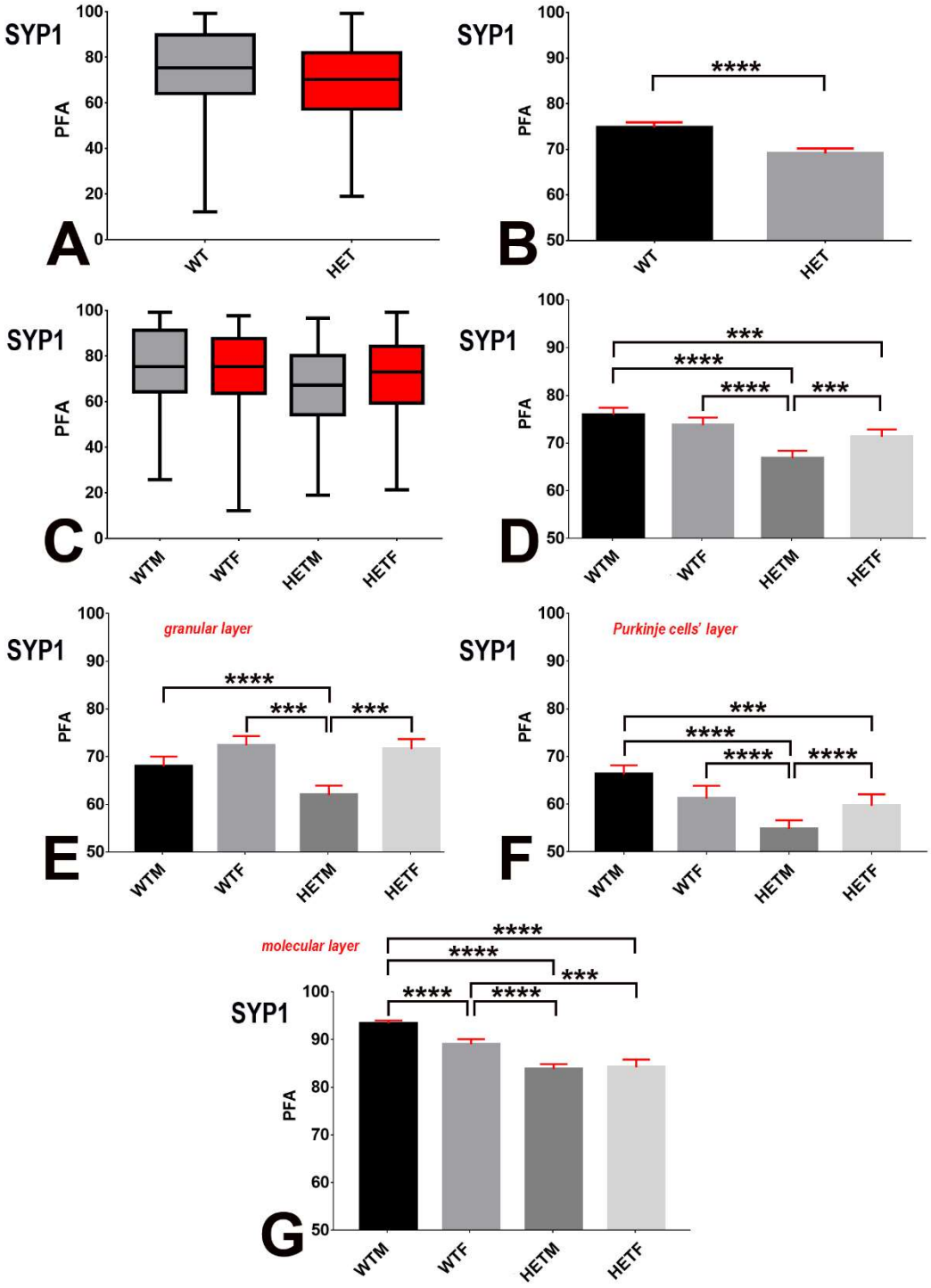

Fig. 4 Statistics of the expression of SYP1 in the cerebellar vermis

A-**B**: Exploratory data analysis (**A**) and inferential statistics (**B**) on whole cerebella after grouping wild-type and heterozygous mice irrespectively of sex. A two-tailed Mann-Whitney test was performed in **B** as data did not pass the D'Agostino & Pearson normality test. **** = P<0.0001; **C**-**D**: exploratory data analysis (**C**) and inferential statistics (**D**) of the four experimental groups defined at beginning of experimental plan. A two-tailed Mann-Whitney test was performed in **D** as data did not pass the D'Agostino & Pearson normality test. **** = P<0.0001, *** 0.0001<P<0.01; **E**-**G**: Kruskal-Wallis test followed by Dunn's multiple comparisons test on PFAs

in the granular layer (**E**), Purkinje cells' layer (**F**) and molecular layer (**G**) of the cerebellar cortex after assessment that data did not pass the D'Agostino & Pearson normality test. **** = P<0.0001, *** 0.0001<P<0.001 (**E-F**) or = 0.0002 (**G**). Outliers were removed in **G**. Bars are 95% CI. Box-and-wisher plots display the range of data (maximum, minimum), the quartiles and the median. *Abbreviations*: F = females; HET = heterozygous; M = males; PFA = percentage of fluorescent area; SYP1 = synaptophysin 1; WT = wild-type.

Comparison between experimental groups

Whole vermis

When PFAs were analyzed in the four experimental groups of this study (Fig. 4C-D), inferential statistics (Fig. 4D) showed that *reln*$^{+/-}$ males displayed a reduction of 11.89% which was statistically significant when compared to wild-type male mice (mean ± CI: wild-type males = 75.86 ± 1.56; *reln*$^{+/-}$ males = 66.84 ± 1.55; Kruskal-Wallis test approximate P value <0.0001 followed by Dunn's multiple comparisons test, adjusted P value <0.0001). Notably, the differences in PFAs between wild-type males and females (mean ± CI: wild-type males = 75.86 ± 1.56; wild-type females = 73.75 ± 1.60) as well as between wild-type females and *reln*$^{+/-}$ females (mean ± CI: wild-type females = 73.75 ± 1.60; *reln*$^{+/-}$ females = 71.31 ± 1.55) were not statistically significant (Dunn's multiple comparisons test, adjusted P values = 0.7020 and 0.1033, respectively). Heterozygous females, instead, displayed a reduction of 6.00% in PFA when compared to wild-type males (mean ± CI: wild-type males = 75.86 ± 1.56; *reln*$^{+/-}$ females = 71.31 ± 1.55; Kruskal-Wallis test, approximate P value <0.0001 followed by Dunn's multiple comparisons test, adjusted P value =0.0005).

We then used the Scheirer Ray Hare test to analyze the effect of the interaction between *reln* genotype and sex on PFA. Results show that the two factors interact in determining the PFA (P values: 0.097 for sex, <0.0001 for *reln* genotype and 0.0001 for interaction).

Cortical layers

We then examined the values of PFA in each of the three layers that form the cerebellar cortex (Fig. 4E-G).

In the granular and Purkinje cells' layers, *reln*$^{+/-}$ males have lower PFAs than all other groups (Fig. 4E-F). In the granular layer of *reln*$^{+/-}$ males, reduction in PFA is of 8.83% *vs reln*$^{+/+}$ males, 14.44% *vs reln*$^{+/+}$ females and 13.49% *vs reln*$^{+/-}$ females. In the Purkinje cells' layer of *reln*$^{+/-}$ males, reduction in PFA is of 17.33% *vs reln*$^{+/+}$ males, 10.49% *vs reln*$^{+/+}$ females and 8.23% vs *reln*$^{+/-}$ females. Notably there were no differences between wild-type males and females (adjusted P value: granular layer = 0.0577; Purkinje cells' layer = 0.0511) and between females of different *reln* genotypes (adjusted P value: granular layer > 0.9999; Purkinje cells' layer = 0.6937). It is also worth noting that, in the Purkinje cells' layer, *reln*$^{+/-}$ females had lower PFA than *reln*$^{+/+}$ males (adjusted P value = 0.0002).

In the molecular layer (Fig. 4G), both *reln*$^{+/-}$ males and females have lower PFAs than wild-type mice of the two sexes. In *reln*$^{+/-}$ males, reduction in PFA is of 10.23% *vs reln*$^{+/+}$ males and 5.84% *vs reln*$^{+/+}$ females. In *reln*$^{+/-}$ females, reduction in PFA is of 9.84% *vs reln*$^{+/+}$ males and 5.43% *vs reln*$^{+/+}$ females. Notably, in this layer there were no differences between *reln*$^{+/-}$ males and *reln*$^{+/-}$ females (adjusted P value = 0.3303).

This set of experiments confirmed that reduction of PFAs was widespread across the three cortical layers in *reln*$^{+/-}$ males and indicated that the *reln* mutation also affects the females but only at the level of the molecular layer and less severely than in males.

Again, we used the Scheirer Ray Hare test to analyze the effect of the interaction between the genotype *(reln*/sex) and the cortical layer on PFA. Results show a statistically significant interaction of the two factors in determining PFAs (P values: <0.0001 for layers, <0.0001 for *reln* genotype and <0.0001 for interaction).

Vermal lobules

We then analyzed the differences in PFA for each vermian lobule. Lobules were identified according to White and Sillotoe (2013) and analysis was first performed considering the whole cortex and then the three cortical layers separately.

Within each of the four experimental groups of the study, PFAs were not statistically different among lobules (Kruskal-Walls test, approximate P values: *reln*$^{+/+}$ males = 0.9913; *reln*$^{+/+}$ females = 0.8165; *reln*$^{+/-}$ males = 0.3184; *reln*$^{+/-}$ females = 0.7103).

The results of the comparisons among experimental groups are described below.

Lobule I

Differences in PFAs among the four experimental groups of this study are reported in Fig.5A. Notably, reln$^{+/-}$ males have lower PFAs than wild-type animals (Dunn's multiple comparisons test, adjusted P values: *reln*$^{+/+}$ males vs *reln*$^{+/-}$ males = 0.0056; *reln*$^{+/+}$ females *vs reln*$^{+/-}$ males = 0.0087) with a reduction of 20.63% *vs* wild-type males and 20.21% *vs* wild-type females.

In the granular layer (Fig. 5C) the PFA in *reln*$^{+/-}$ males is rather only different from that of *reln*$^{+/+}$ females (Tukey's multiple comparisons test adjusted P value = 0.0069) with a reduction of 28.64%.

There were, instead, no statistically significant differences between experimental groups in the Purkinje cells' layer (Kruskal-Wallis test, approximate P value = 0.0338), whereas in the molecular layer (Fig. 6A) the PFA was significantly lower in *reln*$^{+/-}$ males compared to *reln*$^{+/+}$ males (Dunn's multiple comparisons test, adjusted P value = 0.0006) with a reduction of 14.27%.

Lobule II

Fig. 5B shows the differences in PFAs in the four experimental groups of this study. In this lobule, *reln*$^{+/-}$ males have lower PFAs than *reln*$^{+/+}$ males (Dunn's multiple comparisons test, adjusted P value = 0.0097), with a reduction of 15.18%.

When PFAs were compared in the granular layer (Fig. 3D) *reln*$^{+/-}$ males were different from *reln*$^{+/+}$ males (Dunn's multiple comparisons test, adjusted P value = 0.0089) and *reln*$^{+/+}$ females (Dunn's multiple comparisons test, adjusted P value = 0.0016) with reductions of 23.11% and 26.61%, respectively.

There were, instead, no statistically significant differences between experimental groups in the Purkinje cells' layer (Kruskal-Wallis test, approximate P value = 0.2299), whereas in the

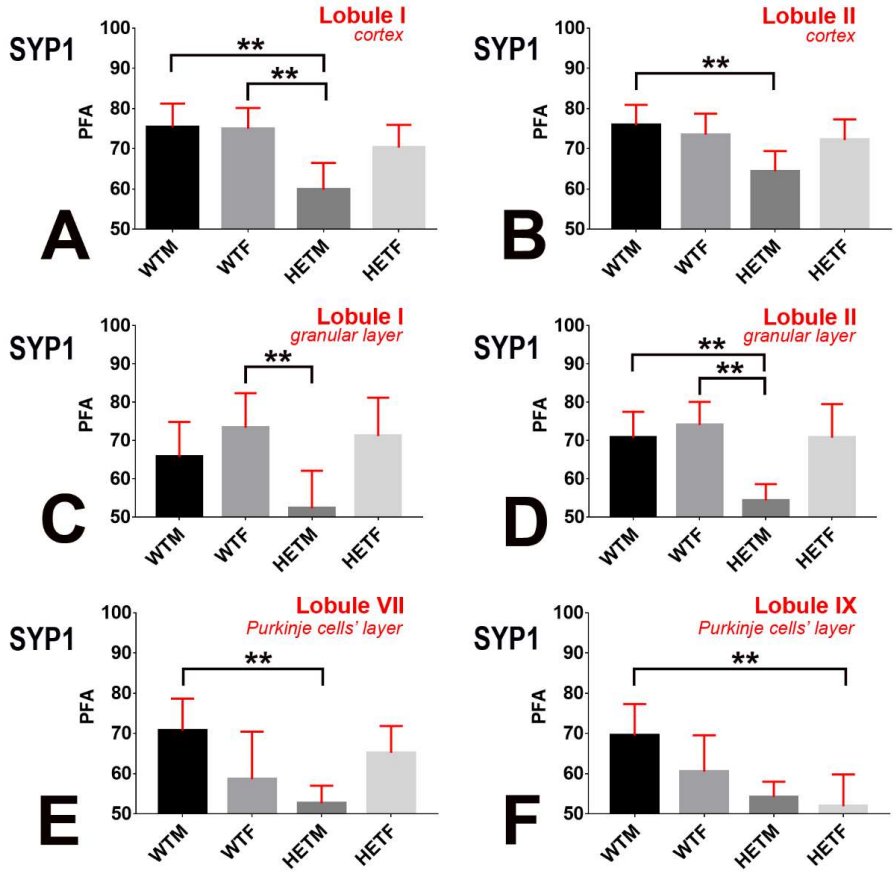

Fig. 5 Differences in the expression of SYP1 in specific lobules of cerebellar vermis among mouse reln genotypes

A-**B**: Kruskal-Wallis test followed by Dunn's multiple comparisons test on PFAs in the cerebellar cortex of vermian lobules I (**A** - ** 0.001<P<0.01) and II (**B** - ** 0.0001<P<0.001).

C, **E**-**F**: Ordinary One-way ANOVA followed by Tukey's multiple comparisons test on PFA in the granular layer of vermian lobule I (**C** - ** 0.001<P<0.01) and in the Purkinje cells' layer of vermian lobules VII (**E** - ** P = 0.0064) and IX (**F** - ** 0.001<P<0.01). **D**: Kruskal-Wallis test followed by Dunn's multiple comparisons test on PFA in the granular layer of vermian lobule II; ** 0.01<P<0.001. Bars are 95% CI. *Abbreviations*: F = females; HET = heterozygous; M = males; PFA = percentage of fluorescent area; SYP1 = synaptophysin 1; WT = wild-type.

molecular layer (Fig. 6B) the PFA was significantly lower in *reln*$^{+/-}$ of both sexes compared to *reln*$^{+/+}$ males (Dunn's multiple comparisons test, adjusted P values: *reln*$^{+/-}$ males *vs* *reln*$^{+/+}$ males = 0.0028; *reln*$^{+/-}$ females *vs* *reln*$^{+/+}$ males = 0.0027), with reductions of 11.65% in *reln*$^{+/-}$ males and 12.33% in *reln*$^{+/-}$ females.

Lobule III

Differences between experimental groups were not statistically significant when the cortex was considered as a whole (Kruskal-Wallis test, approximate P value = 0.1901) as well as in the granular and Purkinje cells' layers (Kruskal-Wallis test, approximate P values = 0.0592 and 0.0730, respectively). In the molecular layer (Fig. 6C), instead, *reln*$^{+/-}$ of both sexes had lower PFAs compared to *reln*$^{+/+}$ males (Dunn's multiple comparisons test, adjusted P values:

reln$^{+/-}$ males *vs* *reln*$^{+/+}$ males = 0.0039; *reln*$^{+/-}$ females *vs* *reln*$^{+/+}$ males <0.0001), with reductions of 7.98% and 13.61% respectively.

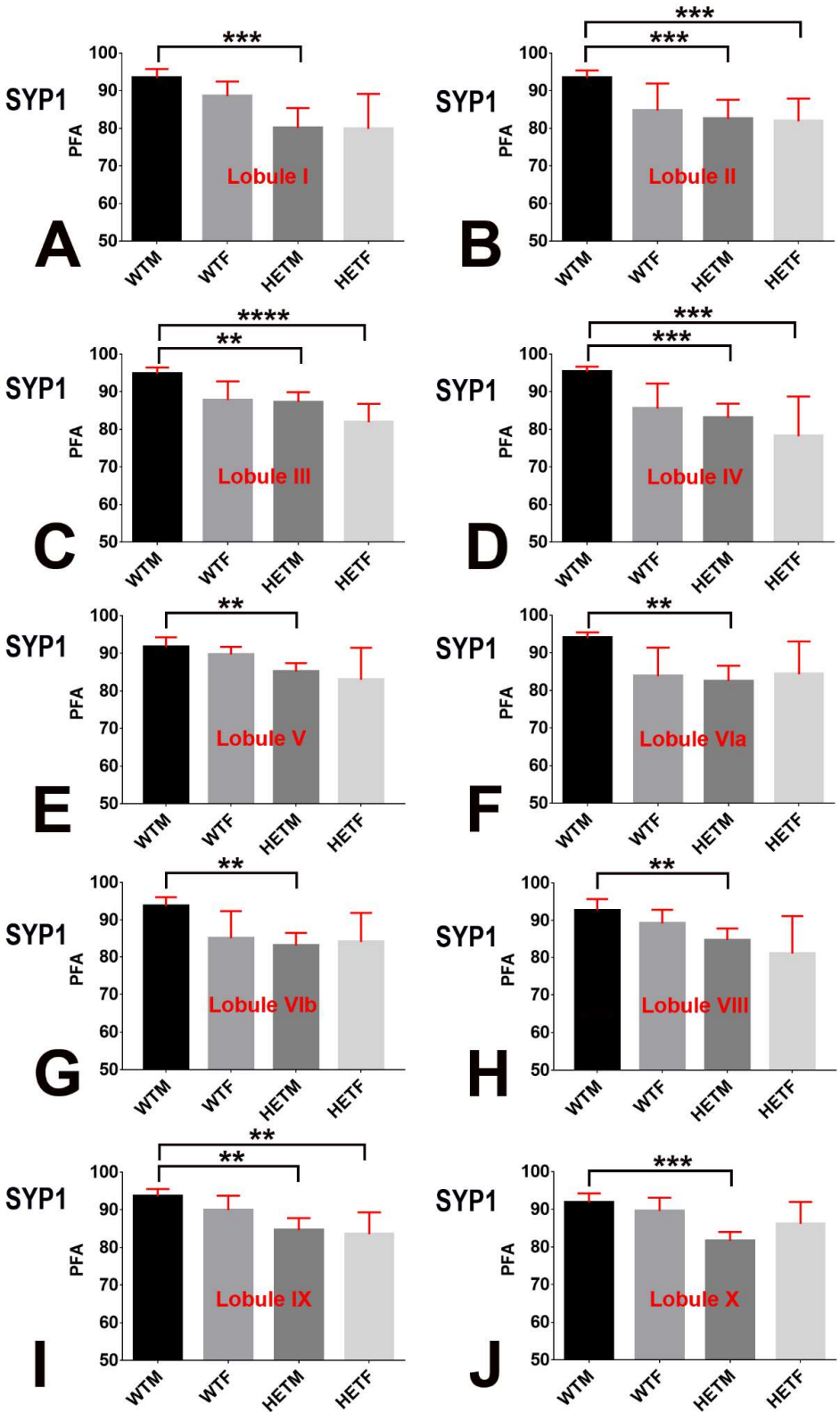

Fig. 6 Expression of SYP1 in the molecular layer of lobules I-X of the cerebellar vermis in different mouse reln genotypes

A-**H**: Kruskal-Wallis test followed by Dunn's multiple comparisons test on PFA in the molecular layer of vermian lobules I (**A** - *** 0.0001<P<0.001), II (**B** *** 0.0001<P<0.001), III (**C** - **** P<0.0001; ** 0.001<P<0.01), IV (**D** - *** 0.0001<P<0.001), V (**E** - ** P = 0.0070), VIa (**F** - ** P = 0.0015), VIb (**G** - ** P = 0.0019) and VIII (**H** - ** P

= 0.0078). **I-J**: Ordinary One-way ANOVA followed by Tukey's multiple comparisons test on PFA in the molecular layer of vermian lobules IX (**I** - ** 0.001<P<0.01) and X (**J** - *** 0.0001<P<0.001). Bars are 95% CI. *Abbreviations*: F = females; HET = heterozygous; M = males; PFA = percentage of fluorescent area; SYP1 = synaptophysin 1; WT = wild-type.

Lobule IV

Also in this lobule differences between experimental groups were not statistically significant when the cortex was considered as a whole (Kruskal-Wallis test, approximate P value = 0.0290), as well as in the granular layer (Kruskal-Wallis test, approximate P value = 0.0124). In the Purkinje cells' layer the difference was significant (Kruskal-Wallis test, approximate P values = 0.0058), but Dunn's multiple comparisons test failed to detect differences between the experimental groups. When the molecular layer was considered (Fig. 6D), instead, *reln*$^{+/-}$ of both sexes had lower PFA compared to *reln*$^{+/+}$ males (Dunn's multiple comparisons test, adjusted P values: *reln*$^{+/-}$ males *vs reln*$^{+/+}$ males = 0.0001; *reln*$^{+/-}$ females *vs reln*$^{+/+}$ males = 0.0005), with reductions of 12.88% and 18.01% respectively.

Lobules V, VIa and VIb

Again, differences between experimental groups were not statistically significant when the cortex was considered as a whole (Kruskal-Wallis test, approximate P values: lobule V = 0.3667; lobule VIa = 0.1887; lobule VIb = 0.1760), as well as in the granular layer [P values: lobule V = 0.3559 (one-way ANOVA); lobule VIa = 0.0336 (approximate - Kruskal-Wallis test); lobule VIb = 0.0704 (one-way ANOVA)] and in the Purkinje cells' layer [P values: lobule V = 0.0819 (approximate - Kruskal-Wallis test); lobule VIa = 0.4822 (one-way ANOVA); lobule VIb = 0.6604 (one-way ANOVA)]. When, instead, the molecular layer was considered (Fig. 6E-G) *reln*$^{+/-}$ males had lower PFA compared to *reln*$^{+/+}$ males (Dunn's multiple comparisons test: Lobule V adjusted P value = 0.0071; Lobule VIa adjusted P value = 0.0015; Lobule VIb adjusted P value = 0.0019). Reductions were of 7.08% (lobule V), 12.24% (lobule VIa) and 11.44% (lobule VIb).

Lobule VII

This lobule did not show any statistically significant difference among the four experimental groups of the study when the cerebellar cortex was considered as a whole (Kruskal-Wallis test, approximate P value = 0.0595) as well as when the granular layer (one-way ANOVA P value = 0.2040) and the molecular layer (one-way ANOVA P value = 0.6673) were analyzed. Notably, in the Purkinje cells' layer (Fig. 5E) there was, instead, a difference in the PFA between males of different *reln* genotypes (adjusted P value = 0.0064) with a reduction of 25.67% in *reln*$^{+/-}$ males.

Lobule VIII

This lobule did not show any statistically significant difference among the four experimental groups of the study when the cerebellar cortex was considered as a whole (one-way ANOVA P value = 0.0267), as well as when the granular layer (one-way ANOVA P value = 0.1949) and Purkinje cells' layer (one-way ANOVA P value = 0.0167) were investigated. In the molecular layer (Fig. 6H) there was a difference in the PFA between males of different *reln*

genotypes (Dunn's multiple comparisons test, adjusted P value = 0.0079), with a reduction of 8.61% in *reln*$^{+/-}$ males.

Lobule IX
This lobule did not show any statistically significant difference among the four experimental groups of the study for the whole cerebellar cortex (Kruskal-Wallis test, approximate P value = 0.0158), as well as when the granular cell layer was considered (one-way ANOVA P value = 0.3140). In the Purkinje layer (Fig. 5F) there was a difference in the PFA between *reln*$^{+/+}$ males and *reln*$^{+/-}$ females (Tukey's multiple comparisons test, adjusted P value = 0.0035), the latter displaying a reduction of 25.29% compared to wild-type males. We also observed a difference in the PFA between wild-type males and *reln*$^{+/-}$ mice of both sexes in the molecular layer (Fig. 6I - Tukey's multiple comparisons test, adjusted P values: *reln*$^{+/+}$ males *vs reln*$^{+/-}$ males = 0.0051; *reln*$^{+/+}$ males *vs reln*$^{+/-}$ females = 0.0014), with a reduction of 9.58% in *reln*$^{+/-}$ males and 10.74% in females.

Lobule X
This lobule did not show any statistically significant difference among the four experimental groups of the study when the cerebella cortex was considered as a whole (Kruskal-Wallis test approximate P value = 0.0442), as well as when the granular layer (one-way ANOVA P value = 0.2107) and Purkinje cells' layer (Kruskal-Wallis test approximate P value = 0.1510) were investigated. There was, instead, a difference in the PFA between *reln*$^{+/+}$ and *reln*$^{+/-}$ males in the molecular layer (Fig. 6J - Tukey's multiple comparisons test, adjusted P value = 0.0006), with a reduction of 11.20% in *reln* heterozygous males.

We used the Scheirer Ray Hare test to analyze the effect of the interaction between the genotype (*reln*/sex) and cerebellar lobules on PFA. Results showed that these factors do not interact in determining the PFA (P value: 0.9258 for lobules, <0.0001 for genotypes and 0.9240 for interaction).
Finally, we have used the Scheirer Ray Hare test to analyze the effect of the interaction between the *reln* genotype/sex and cortical layer in each cerebellar lobule on PFA. Results show that also at the level of the individual layers of the cerebellar cortex there is no interaction with genotype in determining the PFA (granular layer P value: 0.3150 for lobules, <0.0001 for genotypes and 0.5518 for interaction; Purkinje cells layer P value: 0.5170 for lobules, <0.0001 for genotypes and 0.0763 for interaction; molecular layer P value: 0.9448 for lobules, <0.0001 for genotypes and 0.9710 for interaction).

Quantitative analysis of CNTN6 immunofluorescence

Again, before comparing the four experimental groups of this study we have verified the absence of statistically significant differences between animals of the same genotype. In this case, we have investigated CNTN6 immunoreactivity in the whole vermis and the single cortical layers.

Whole vermis

Males vs females

When the cerebellar vermis of males and females were compared irrespectively of the *reln* genotype, the means of PFA were not statistically different in the two groups (mean ± CI: males = 77.66 ±3.40; females: 79.68 ± 3.51; two-tailed Mann-Whitney test P =0.2074).

Wild-type vs heterozygous mice

Fig. 7A shows the exploratory data analysis of the vermis of wild-type and heterozygous mice. When wild-type and heterozygous *reln*$^{+/-}$ mice were compared irrespectively of sex (Fig. 7B), the two groups were statistically different (mean ± CI: *reln*$^{+/+}$ = 87.72 ± 2.24; *reln*$^{+/-}$: 70.05 ± 3.52; two-tailed Mann-Whitney test P<0.0001). Specifically, *reln*$^{+/-}$ mice displayed a reduction of 20.14% in PFA compared to wild-type mice.

Comparison between experimental groups

Whole vermis

When PFAs were analyzed in the four experimental groups of this study (Fig. 7C-D), inferential statistics (Fig. 7D) showed that *reln*$^{+/-}$ males displayed a reduction of 18.85% compared to wild-type male mice (mean ± CI: *reln*$^{+/+}$ males = 85.25 ± 2.94; *reln*$^{+/-}$ males = 69.18 ± 3.68; Kruskal-Wallis test approximate P value <0.0001 followed by Dunn's multiple comparisons test, adjusted P value <0.0001) and a reduction of 20.00 % compared to wild-type female mice (mean ± CI: *reln*$^{+/-}$ males = 69.18 ± 3.68; *reln*$^{+/+}$ females = 86.47 ± 2.84; Kruskal-Wallis test approximate P value <0.0001 followed by Dunn's multiple comparisons test, adjusted P value <0.0001). Similarly, *reln*$^{+/-}$ females displayed a reduction of 17.97% compared to wild-type females (mean ± CI: *reln*$^{+/+}$ females = 86.47 ± 2.84; *reln*$^{+/-}$ females = 70.93 ± 3.92; Kruskal-Wallis test approximate P value <0.0001 followed by Dunn's multiple comparisons test, adjusted P value <0.0001) and a reduction of 16.80% compared to wild-type male mice (mean ± CI: *reln*$^{+/+}$ males = 85.25 ± 2.94; *reln*$^{+/-}$ females = 70.93 ± 3.92; Kruskal-Wallis test approximate P value <0.0001 followed by Dunn's multiple comparisons test, adjusted P value <0.0001).

Notably, the differences in PFAs between mice of the same genotype but different sex were not statistically significant (mean ± CI: *reln*$^{+/+}$ males = 85.25 ± 2.94, *reln*$^{+/+}$ females = 86.47 ± 2.84; Dunn's multiple comparisons test, adjusted P value >0.9999 and mean ± CI: *reln*$^{+/-}$ males = 69.18 ± 3.68, *reln*$^{+/-}$ females = 70.93 ± 3.92; Dunn's multiple comparisons test, adjusted P value >0.9999).

We then used the Scheirer Ray Hare test to analyze the effect of the interaction between *reln* genotype and sex on PFA. Results show that the two factors do not interact in determining the PFA (P values: 0.407 for sex, 5.22E-17 for *reln* genotype and 0.8593 for interaction).

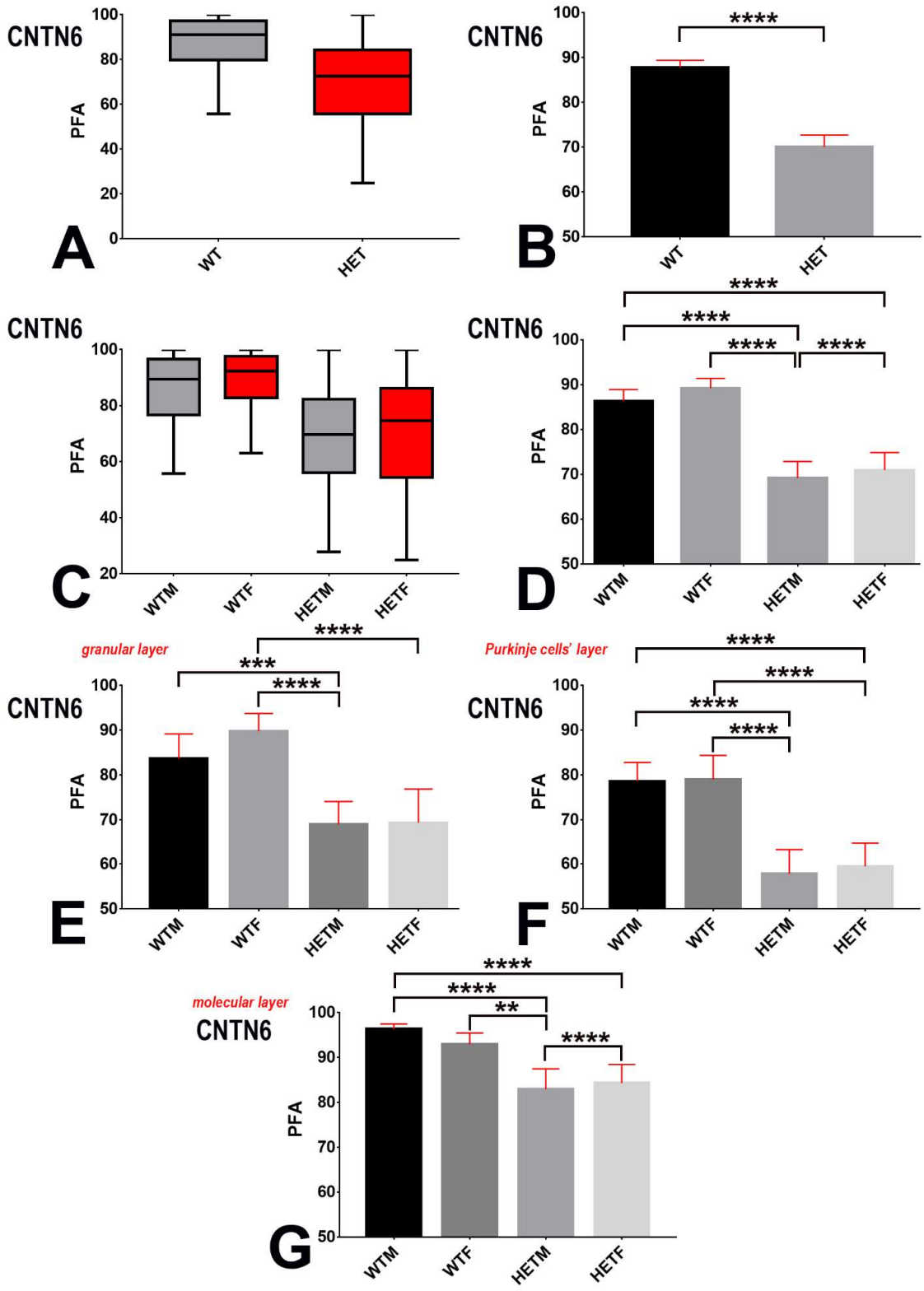

Fig. 7 Statistics of the expression of CNTN6 in the cerebellar vermis

A-**B**: Exploratory data analysis (**A**) and inferential statistics (**B**) on whole cerebella after grouping wild-type and heterozygous mice irrespectively of sex. A two-tailed Mann-Whitney test was performed in **B** as data did not pass the D'Agostino & Pearson normality test. **** = P<0.0001; **C**-**D**: exploratory data analysis (**C**) and inferential statistics (**D**) of the four experimental groups defined at beginning of experimental plan. A two-tailed Mann-Whitney test was performed in **D** as data did not pass the D'Agostino & Pearson normality test. **** = P<0.0001, *** 0.0001<P<0.01; **E**-**G**: Kruskal-Wallis test followed by Dunn's multiple comparisons test on PFAs

in the granular layer (**E**), Purkinje cells' layer (**F**) and molecular layer (**G**) of the cerebellar cortex after assessment that data did not pass the D'Agostino & Pearson normality test. **** = P<0.0001, *** 0.0001<P<0.001 (**E-F**) or = 0.0002 (**G**). Outliers were removed in **G**. Bars are 95% CI. Box-and-wisher plots display the range of data (maximum, minimum), the quartiles and the median. *Abbreviations*: CNTN6 = contactin 6; F = females; HET = heterozygous; M = males; PFA = percentage of fluorescent area; WT = wild-type.

Cortical layers

We then examined the values of PFA in each of the three layers that form the cerebellar cortex (Fig. 7E-G).

In the granular layer (Fig. 7E) of *reln*$^{+/-}$ males, reduction in PFA is of 17.53% *vs reln*$^{+/+}$ males, and 23.12% *vs reln*$^{+/+}$ females (mean ± CI: *reln*$^{+/-}$ males = 68.93 ± 5.14; *reln*$^{+/+}$ males = 83.66 ± 5.49; Kruskal-Wallis test approximate P value <0.0001 followed by Dunn's multiple comparisons test, adjusted P value <0.0019; mean ± CI: *reln*$^{+/-}$ males = 68.93 ± 5.14; *reln*$^{+/+}$ females = 89.74 ± 4.03; Kruskal-Wallis test approximate P value <0.0001 followed by Dunn's multiple comparisons test, adjusted P value <0.0001). In addition, in this layer *reln*$^{+/-}$ females display a 22.70% reduction in PFA *vs reln*$^{+/+}$ females (mean ± CI: *reln*$^{+/-}$ females = 69.37 ± 7.50; *reln*$^{+/+}$ females = 89.74 ± 4.03; Kruskal-Wallis test approximate P value <0.0001 followed by Dunn's multiple comparisons test, adjusted P value <0.0001). The 17.08% reduction of PFA in *reln*$^{+/-}$ females compared to *reln*$^{+/+}$ males is instead just below the P value set for statistical significance (mean ± CI: *reln*$^{+/-}$ females = 69.37 ± 7.50; *reln*$^{+/+}$ males = 83.66 ± 5.49; Kruskal-Wallis test approximate P value <0.0001 followed by Dunn's multiple comparisons test, adjusted P value 0.0198).

In the Purkinje cell layer (Fig. 7F) of *reln*$^{+/-}$ males, reduction in PFA is of 26.47% *vs reln*$^{+/+}$ males, and 26.82% *vs reln*$^{+/+}$ females (mean ± CI: *reln*$^{+/-}$ males = 57.80 ± 5.55; *reln*$^{+/+}$ males = 78.60 ± 4.16; Kruskal-Wallis test approximate P value <0.0001 followed by Dunn's multiple comparisons test, adjusted P value <0.0001; mean ± CI: *reln*$^{+/-}$ males = 57.80 ± 5.55; *reln*$^{+/+}$ females = 78.98 ± 5.37; Kruskal-Wallis test approximate P value <0.0001 followed by Dunn's multiple comparisons test, adjusted P value <0.0001). Also, in this layer *reln*$^{+/-}$ females display a 24.35 % reduction in PFA *vs reln*$^{+/+}$ males (mean ± CI: *reln*$^{+/-}$ females = 59.46 ± 5.34; *reln*$^{+/+}$ males = 78.60 ± 4.16; Kruskal-Wallis test approximate P value <0.0001 followed by Dunn's multiple comparisons test, adjusted P value <0.0001) and a 24,71% reduction in PFA *vs reln*$^{+/+}$ females (mean ± CI: *reln*$^{+/-}$ females = 59.46 ± 5.34; *reln*$^{+/+}$ females = 78.98 ± 5.37; Kruskal-Wallis test approximate P value <0.0001 followed by Dunn's multiple comparisons test, adjusted P value <0.0001).

In the molecular layer (Fig. 7G) of *reln*$^{+/-}$ males, reduction in PFA is of 13.90 % *vs reln*$^{+/+}$ males, and 10.79% *vs reln*$^{+/+}$ females (mean ± CI: *reln*$^{+/-}$ males = 82.90 ± 4.57; *reln*$^{+/+}$ males = 96.30 ± 1.17; Kruskal-Wallis test approximate P value <0.0001 followed by Dunn's multiple comparisons test, adjusted P value <0.0001; mean ± CI: *reln*$^{+/-}$ males = 82.90 ± 4.57; *reln*$^{+/+}$ females = 92.93 ± 2.51; Kruskal-Wallis test approximate P value <0.0001 followed by Dunn's multiple comparisons test, adjusted P value 0.0044). In this layer too, *reln*$^{+/-}$ females display a 12.5% reduction in PFA *vs reln*$^{+/+}$ males (mean ± CI: *reln*$^{+/-}$ females = 84.26 ± 4.15; *reln*$^{+/+}$ males = 96.30 ± 1.17; Kruskal-Wallis test approximate P value <0.0001 followed by Dunn's

multiple comparisons test, adjusted P value <0.0001) and a 9.34% reduction in PFA *vs* *reln*$^{+/+}$ females (mean ± CI: *reln*$^{+/-}$ females = 84.26 ± 4.15; *reln*$^{+/+}$ females = 92.93 ± 2.51; Kruskal-Wallis test approximate P value <0.0001 followed by Dunn's multiple comparisons test, adjusted P value 0.0127).
From this set of experiments showed one can conclude that in all cortical layers, *reln*$^{+/-}$ mice have lower PFAs than *reln*$^{+/+}$ mice, whereas there are no sex-related differences between mice of the same genotype. These observations are in line with the results of the Scheirer Ray Hare test that demonstrated no interaction between the genotype *(reln*/sex) and the cortical layer in determining PFA (P values: genotype = 5.17E-15; layer = 1.37E-17; interaction = 0.955921).

Discussion

The autistic cerebellum displays several histological alterations that have been recently considered in a consensus paper (Fatemi et al. 2012) and *RELN* was associated to autism and its cerebellar pathology (Fatemi 2005; Hong et al. 2000; Lammert and Howell, 2016).
We have here demonstrated a reduction in the levels of expression of SYP1 and CNTN6 in the cerebellar vermis of the heterozygous *Reeler* mouse, a putative translational model for human autism. In the following, we will first discuss our findings in relation to the possible modifications of the cerebellar connections in these mice, as a consequence of reelin haplodeficiency. Then, we will consider whether or not these modifications relate to those observed in the autistic cerebellum. Finally, we will briefly discuss synaptic alterations in other animal models of autism.

Alterations in the cerebellar vermis of the reln$^{+/-}$ *mouse*
Does gender influence the structural phenotype of the heterozygous Reeler mice?
In the vermian cortex, we here show that *reln*$^{+/-}$ males display a statistically significant diminution in the expression of SYP1 (Fig. 4D) and CNTN6 (Fig. 7D) compared to sex-matched wild-type animals. In addition, when the *reln* genotype and sex were considered as two independent factors, they displayed a statistically significant interaction in determining the reduction of vermian SYP1 (Scheirer Ray Hare test P = 0.000106), but not of CNTN6 (Scheirer Ray Hare test P = 0.8593). Therefore, it appears that the mutated genotype is the main factor responsible for the structural modifications in the cerebellar vermis that we have observed here, although the expression of SYP1 also seems to be influenced by sex.
Wild-type mice (and rats) are known to display some sexual dimorphic features of their cerebella (Dean and McCarthy 2008; Mercer at al. 2016; Abel et al. 2011). Therefore, the effect of gender in determining the response to gene mutations should not be underestimated. Notably, dimorphic features were recently observed in relation to the physiology of synapses in the *Gabrb3* heterozygous mouse, another autism-linked mutant (Mercer et al. 2016). In these animals the electrophysiological responses recorded from the neurons of the cerebellar nuclei were different between the two sexes. However, heterozygous mice did not display gender-related behavioral differences at the rotaroid task. Thus, the electrophysiological changes observed in males were interpreted to be

compensatory (Mercer et al. 2016), a possibility that one should take into consideration when explaining the structural changes in the vermis of the heterozygous *Reeler* mice that we and others have observed previously. In former studies there were no gender-related differences in the number and topology of the Purkinje neurons in wild-type mice (Magliaro et al. 2016), but *reln*$^{+/-}$ males and not females had less Purkinje neurons than sex-matched *reln*$^{+/+}$ subjects (Magliaro et al. 2016; Biamonte et al. 2009; Hadj-Sahraoui et al. 1996). Intriguingly, we observed that both *reln*$^{+/-}$ males and females had reduced numbers of Purkinje neurons than wild-type males, and that such a reduction was more evident in *reln*$^{+/-}$ females (17.73%) than males (14.37%) (Magliaro et al. 2016). Similarly, we here detected that, in multiple comparison tests, there was not a statistically significant difference in the expression of SYP1 and CNTN6 between wild-type males and females, but that heterozygous mice of both sexes had lower levels of expression than wild-type males with a reduction of 11.89% in males and 6.00% in females for SYP1 and of 18.85% in males and 20.00% in females for CNTN6. After Mann-Whitney test, there was a very strong statistically significant difference between males and females of different genotypes for CNTN6 but only between males for SYP1 (two-tailed approximate P value <0.0001). As to the latter, when the females of the two genotypes were compared the two-tailed approximate P was 0.0126, a value only slightly higher than the predetermined threshold of our experiments. A *post-hoc* computed power of the Mann-Whitey test (two groups) for SYP1 gave the following values (size of groups = 396): males - α error probability 0.01; effect size 0.5726980; power (1-β error probability) 0.999995; females - α error probability 0.01; effect size 0.1263960; power (1-β error probability) 0.1770646. These observations indicated that the *reln* mutation has an impact on the level of expression of SYP1 in both male and female mice, but, in the latter, the effect size is clearly much reduced. That reelin haplodeficiency also impacts in females is, on the other hand, well demonstrated after analysis of CNTN6 immunostaining.

As pre-planned, our SYP1 statistics had a quite high probability (17.7%) for type II error (false negatives) to occur in females. Thus, we cannot exclude that a different sampling strategy could unravel more subtle effects of the reelin haplodeficiency in females. However, if one computes *a priori* the required sample size to achieve a power of 0.9999, given the same α error probability and effect size calculated after *post-hoc* computation, the required size of groups would be 3865, a figure that obviously conflicts with the 3Rs principles on ethical use of animals in biomedical research.

Nonetheless, in keeping with our findings, it was demonstrated that 17β-estradiol upregulated the reelin mRNA only in the cerebellum of *reln*$^{+/-}$ male mice, this providing support to the existence of gender-dependent differences in the vulnerability to the mutation (Biamonte et al. 2009).

Reln heterozygous mice have cortical layer-specific reductions in SYP1 expression and a layer-diffuse decrease of CNTN6 immunoreactivity

Considering SYP1, differences between wild-type males and females are not statistically significant in the granular and Purkinje cells' layers, but wild-type females have a lower level of expression than wild-type males in the molecular layer (Fig. 4G). CNTN6 does not, instead, show different cortical levels of expression between the two sexes (Fig. 7G). Therefore, it may be the molecular layer to offer a different baseline for the mutation.

As regarding the heterozygous mice, males only have statistically significant reduced levels of SYP1 expression in the granular cell layer (Fig. 4E), both males and females display lower levels than wild-type males in the Purkinje cells' layer (Fig. 4F), whereas in the molecular layer, both males and females have lower PFAs than wild-type mice of the two sexes (Fig. 4G). In *reln*$^{+/-}$ males, reduction in molecular layer PFA is of 10.23% *vs reln*$^{+/+}$ males and 5.84% *vs reln*$^{+/+}$ females. In *reln*$^{+/-}$ females, reduction in PFA is of 9.84% *vs reln*$^{+/+}$ males and 5.43% *vs reln*$^{+/+}$ females.
Thus, also a layer-centered analysis converged to indicate that reelin haplodeficiency led to structural changes in females as well, although less severely than in males. In addition, this type of analysis showed that reduction of SYP1 is widespread across the three cortical layers in *reln*$^{+/-}$ males but restricted to the molecular layer in *reln*$^{+/-}$ females.
When cortical layers were considered separately, the impact of the mutation on CNTN6 is more widespread, as it affects heterozygous mice of both sexes and the decrease in the levels of expression is higher: about 17-23% in the granular layer, 24-26% in the Purkinje cell layer, and 9-14% in the molecular layer (Fig. 7).

A very limited number of biochemical and immunochemical studies have analyzed the levels of expression of synaptic proteins in *reln*$^{+/-}$ mice, whereas there are no histological reports on this issue, at least to the best of our knowledge. Similarly, there are no data on the expression of CNTN6 in homozygous and heterozygous mutants. After ELISA, unaltered levels of several presynaptic proteins, including SYP1, were described in the frontal cortex, hippocampus and cerebellum of heterozygous male mice compared to wild-type animals of the same sex, but authors themselves were puzzled by this finding (Barr et al. 2008). In another study on hippocampus, adult heterozygous *Reeler* mice of both sexes were compared to wild-type littermates, and specific postsynaptic defects in scaffolding proteins, neurotransmitter receptors and signaling proteins were described in Western blots (Ventruti et al. 2011). The same authors reported that only a modest reduction of spine density in hippocampal area CA1 could be detected by confocal microscopy. In a more recent proteomic study on cerebellum, anterior cingulate cortex, striatum, the hippocampal dentate gyrus and CA3 of male mice, the expression of several cytoskeletal proteins resulted to be affected by the mutation (Schmitt et al. 2013). Of these proteins, the authors considered of particular relevance Hspa8 that is involved in the removal of clathrin-coated vesicles and thus, likely, regulates fast synaptic transmission. This study employed a combination of two-dimensional gel electrophoresis, matrix-assisted laser desorption/ionization-tandem time of flight mass spectrometry, and Western blotting, highlighting the necessity of a very sophisticated approach for the detection of the subtle alterations in heterozygous mutants. Though few and very different in the approaches, these observations and the present work converge to indicate that, despite being difficult to detect, there are indeed neurochemical differences at brain synapses of *reln* heterozygous mice. In keeping with this possibility, we here show that expression of CNTN6, a cell adhesion molecule that intervenes in synaptogenesis (Stoeckli 2010), is severely reduced in *reln*$^{+/-}$ mice. Notably, CNTN6 contributes to the formation of synapses between the parallel fibers and the Purkinje neurons (Sakurai et al. 2009), and the adhesion molecule CNTN1, which appears earlier in development to be then replaced by CNTN6, is expressed by the Golgi cells and the mossy

fibers at cerebellar glomeruli (Falk et al. 2002). Qualitatively, the pattern of expression of CNTN6 that we have described here is in full agreement with these observations. Quantitatively, the widespread reduction in CNTN6 immunoreactivity that in this work we have observed in *reln*$^{+/-}$ mice is also in line with the aforementioned literature: thus in the molecular layer decrease in PFA can be explained by a numerical reduction of the parallel fiber-to-Purkinje neuron (PF-PN) synapses, and in the Purkinje cell layer by the loss of the Golgi cells' dendrites that follows an aberrant distribution restricted to the granular layer (see Fig. 1A in Falk et al. 2002). In the latter, we can speculate that reduction of CNTN6 in heterozygous mice follows a numerical reduction in the population of the Golgi cells, which we have previously demonstrated to undergo a dark-type degeneration in *reln*$^{-/-}$ mice (Castagna et al. 2016), and/or a decrease/alteration in the mossy fibers' afferent system, as heterologous synaptic junctions were demonstrated in homozygous mutants (Wilson et al. 1981).

Alterations in the levels of expression of SYP1 in the molecular layer of male reln$^{+/-}$ *mice are spread across vermian lobules except lobule VII*

Only in lobules I and II there were statistically significant diminutions of PFA affecting *reln*$^{+/-}$ males. In lobule I, reductions were of 20.63% *vs reln*$^{+/+}$ males or 20.21% *vs reln*$^{+/+}$ females. In lobule II, depletion was of 15.8% compared to *reln*$^{+/+}$ males. Differences between experimental groups were not statistically significant for all other lobules.

However, when the single cortical layers were considered, there was a widespread reduction in the degree of expression of SYP1 in the molecular layer of *reln*$^{+/-}$ males *vs reln*$^{+/+}$ males (in lobules I-VI and VIII-X), *reln*$^{+/+}$ females (lobule I) or *reln*$^{+/-}$ females (lobules II-IV and IX). In particular, reductions in the percentages of expression between wild type and haplodeficient males were 14.27% in lobule I, 11.65% in lobule II, 7.98% in lobule III, 12.88% in lobule IV, 7.08% in lobule V, 12.24% in lobule VIa, 11.44% in lobule VIb, 8.61% in lobule VIII, 9.58% in lobule IX and 11.20% in lobule X. The means of SYP1 depletion calculated after analysis of individual lobules or the whole vermis were very close (10.81% and 10.69%, respectively), this observation confirming that the molecular layer is a primary target of the mutation, as also follows the layer-centered analysis of CNTN6 distribution.

Alterations in the levels of expression of SYP1 are restricted to lobule II for the granular layer and lobule VII for the Purkinje cells' layer.

Based on the paucity of data in the literature, reduction of SYP1 expression in specific cortical layers of certain lobules needs to be interpreted with extreme caution, although indicative that reelin haplodeficiency has a large effect in these lobules.

Reln$^{+/-}$ males displayed reduced values of PFAs *vs* wild-type males (23.11%) or females (26.61%) in the granular layer of lobule II and *vs reln*$^{+/+}$ males (25.67%) in the Purkinje cells' layer of lobule VII. The granular layer mainly contains the synapses formed by the cerebellar mossy fibers, whereas the majority of those in the Purkinje cells' layer derive from the basket cells that modulate the inhibitory activity of the Purkinje neurons and occur on both dendritic shafts and the cell body. The density of the two types of synapses was strongly reduced in *reln*$^{-/-}$ mice after ultrastructural examination (Castagna et al. 2014), again providing indirect support to our present observations.

The PF-PN synapses in the *reln*$^{+/-}$ mouse

Most synapses in the molecular layer are made by the parallel fibers, *i.e.* the axons of the granule cells that contact the dendritic trees of the Purkinje neurons with a ratio of 200,000:1 compared to the climbing fibers (Hansel et al. 2001). Therefore, a reduction in the content of presynaptic proteins in this cortical layer could be indicative of a dysfunction of PF-PN synapses. Since our approach did not permit to calculate directly the number of synapses, it was not possible to establish whether reduction in presynaptic SYP1 was related to a decrease in the number of the PF-PN synapses and/or a reduction in the number of synaptic vesicles in the presence of a normally sized synaptic population. However, as in the molecular layer CNTN6 is specifically expressed at these synapses (Stoeckli 2010) and is reduced in heterozygous mice in percentages very close (9-14%) to those above mentioned for SYP1 the first possibility appears to be more realistic. It would also be in line with our ultrastructural observations on homozygous Reeler mice, which displayed, among others, a diminution of about 1/3 in the density of the PF-PN synaptic contacts (Castagna et al. 2014). The second possibility seems to be more difficult to reconcile with the currently accepted quantal hypothesis for transmitter release from (small-sized) synaptic vesicles (Burgoyne and Barclay 2002). Indeed, according to the quantal hypothesis, quantal size (amount of transmitter released per vesicle) is constant. Therefore, if less SYP1 is expressed at a given synapse and a lower number of vesicles are herein contained, less neurotransmitter would be released upon stimulation with obvious consequences on synaptic physiology. The final result would specifically be a depression of the amplitude of miniature EPSCs recorded from the Purkinje neurons, with an impact onto cerebellar LTD (Murashima and Hirano 1999). Unfortunately, there are no electrophysiological recordings on the Purkinje neurons from *reln*$^{+/-}$ mice, and recording from *reln*$^{-/-}$ mice only investigated the properties of the Purkinje neuron-to-climbing fiber synapse (Mariani et al. 1977).

It is also tempting to speculate that reduction of SYP1 and CNTN6 at the PF-PN synapses has an impact on the silent fraction of these synapses. In cerebellum, it was demonstrated that the majority of the PF-PN synapses are electrically silent (Ekerot and Jörntell 2001). It was also hypothesized that silent synapses are produced functionally by LTD, and that learning converts silent synapses to active synapses, or *vice versa*, by the induction of LTP or LTD (Ekerot and Jörntell 2003). PF-PN synapses are known to undergo presynaptic LTP *in vivo*, and a study has demonstrated that silent synapses are indeed activated in cultured cerebellar granule cells after electrical stimulation (Cousin and Evans, 2011). In addition, very recent observations have shown that mice deficient in Lrfn2, a protein of the post-synaptic density that is associated with human autism (Voineagu et al. 2011), display autistic behaviors specifically related to an increment of the silent synapses' pool (Morimura et al. 2017).

Are the reln$^{+/-}$ *mice good models for autism translational studies?*

In the last years, several reviews have discussed the current literature on the mouse models of autisms (Ecker et al. 2013; Bey and Jiang 2014; Halladay et al. 2009; Tsai 2016; Robertson and Feng 2011). According to Robertson and Feng (2011), establishing a good

translational mouse model for a neuropsychiatric disorder requires face, construct and predictive validity.
Strictly speaking, construct validity only applies to transgenic mice but, in a broader sense, it also encompasses the spontaneous mutations affecting the DNA, such is the case of *Reeler*. In other words, this parameter defines the resemblance of the pathology between the mouse and human conditions in terms of the causative gene(s) as *e.g.* inferred from gene association and linkage studies. There is evidence for genetics to be implicated in the etiology of autism but, as a consequence of its multifaceted clinical symptoms, the causative gene(s) remain to be discovered (Miles 2011). Nonetheless, *RELN* is one of the genes associated with the human cerebellar pathology (see Table 1 in Fatemi et al. 2012). Therefore, *Reeler* heterozygous mice reasonably fulfil the construct criterion.
Predictive validity, *i.e.* the resemblance of the response to treatment in the two species, can hardly be assessed, in the absence of an established therapy for the human condition.
Thus, in the context of this discussion, face validity, *i.e.* the resemblance of the model phenotype to that of the human disorder, is the most important parameter to be considered. There are two main streams along which face validity of the *reln*$^{+/-}$ mouse in translational studies on autism can be addressed properly, *i.e.* the validity of the behavioral phenotype and that of the structural phenotype.
As mentioned in the Introduction, there are conflicting views as regarding the recapitulation of the human alterations in the *reln*$^{+/-}$ mouse behavior. This is somewhat not surprising as only a few behavioral tests, such as *e.g.* pre-pulse inhibition (PPI), which measures sensory-motor responses, can be executed in both humans and mice (Geyer 2008). *Reln*$^{+/-}$ mice display decreased PPI, reduced odor discrimination, less anxiety in the elevated plus maze and impaired conditional fear in the active avoidance test in some studies (Tueting et al. 1999; Marrone et al. 2006) but not in others (Salinger et al. 2003; Podhorna and Didriksen 2004; Krueger et al. 2006). Therefore, it becomes very important to properly compare the structural alterations in the brains of the two species to validate or invalidate the model.

<u>The widespread reduction of the presynaptic marker SYP1 in the molecular layer of heterozygous male mice and of the PF-PN synapses' marker CNTN6 is compatible with the human autistic phenotype</u>

In the vermis (and cerebellum in general), there is evidence for a topographic organization of motor control versus cognitive and affective processing, and the different lobules are connected with specific areas of the brain and spinal cord (Stoodley and Schmahmann 2010): CNS areas that process sensorimotor information are directly or indirectly linked with the cerebellar anterior lobe (vermian lobules I–V), lobule VIII, and, to a smaller degree, with lobule VI; in contrast, cerebral association areas that receive non-motor inputs target lobules VI and VII.

Available clinical evidence indicates that the cerebellar vermis is the main target of limbic-related structures, and physiological and behavioral studies support the role of the vermis in the modulation of emotions (Schmahmann et al. 2007). Therefore, the widespread reduction of SYP1 expression in all vermian lobules (except lobule VII) that we here observed in heterozygous male mice (Fig. 6) and the decrease of CNTN6 in all cortical layers of

heterozygous mice of both sexes well correlates with the suggestion that the social and communication abnormalities typically found in autism depend on abnormalities in the limbic structures and their connectivity (Catani et al. 2013).

At autopsy, a loss of Purkinje neurons in the posterior cerebellum was described in autistic patients (Bauman and Kemper 1985; Bauman 1991), but it appeared that such a loss did not affect the vermis, as then reported by Bauman and Kemper in Fatemi et al. (2012). Hypoplasia in lobules VI and VII was first observed *in vivo* after neuroimaging (Courchesne et al. 1988), but later work provided evidence of two distinct autistic subtypes associated with vermian hypoplasia or hyperplasia (Courchesne et al. 1994). A systematic review and meta-analysis of structural magnetic resonance imaging (sMRI) studies has then demonstrated that the decrease in size of vermian lobules VI-X (*i.e.* the lobules comprised in the posterior cerebellum) displayed a notable heterogeneity that correlated to differences in age and intelligence quotient (IQ) of the study population only in lobules VI-VII (Stanfield et al. 2008). Other more recent studies on the autistic cerebellum indicated that the posterior/inferior vermis was more susceptible to undergo pathological changes (Limperopoulos et al. 2007), and lobules VII, VIIIb (left) and IX were implicated with a reduction of the gray matter after quantitative imaging of autistic patients (D'Mello and Stoodley 2015; Stoodley 2014; D'Mello et al. 2015). Therefore, while sMRI findings on the posterior cerebellum should be interpreted with great caution, experimental evidence supports the notion that the cerebellar vermis is somewhat altered in autistic patients with a certain degree of hypoplasia that depends from a decrease in cortical (gray matter) volume. Therefore, the neurochemical alterations of the molecular layer that we observed here in *reln*$^{+/-}$ mice are fully compatible with the human pathology. In addition, the recent accumulation of data showing *CNTN6* mutations are a risk factor for autism (see e.g. Hu et al 2015, Mercati et al 2017, Oguro-Ando et al 2017) give further weight to the use of *reln* heterozygous mice as translational models for the disease.

<u>Alterations in the level of expression of SYP1 in lobule II granular layer do not find an equivalent in the functional autistic phenotype</u>

Reln$^{+/-}$ males displayed reduced values of PFAs *vs* wild-type males or females in the granular layer of lobule II. As synapses in the granular layer mainly occur at the mossy fibers' rosettes, this observation supports the possibility that a reduced afferent input exists to this lobule. However, when resting-state functional magnetic resonance imaging was used to define the subregions of the cerebellar cortex functionally connected to the prefrontal, motor, somatosensory, posterior parietal, visual, and auditory cortices in healthy volunteers, the entire vermis did not show significant correlation with any mask of the study (O'Reilly et al. 2010). In keeping with these observations, previous animal studies have demonstrated that lobules I-II receive afferents from the spinal cord (see *e.g.* Matsushita and Okado 1981). Therefore, the differences here observed in the heterozygous males are difficult to be linked with the autistic phenotype and need to be confirmed by further studies.

<u>Alterations in the level of expression of SYP1 in lobule VII Purkinje cells' layer are consistent with the human autistic phenotype</u>

The lobule VII of the *reln*$^{+/-}$ male mice displayed unique features that were limited to a reduction in the SYP1 content of the Purkinje cells' layer (Fig. 5E), whereas there were no alterations in the molecular layer. The human lobule VII is activated during cognitive tasks and receives a very specific input from the principal inferior olivary nucleus (see Stoodley and Schmahmann 2010 for review). Transcranial magnetic stimulation of vermian lobule VII influenced the cerebral dorsal attention system (Halko et al. 2014). Recently, Suzuki et al. have employed retrograde tracing with rabies virus to study the organization of the cerebral projections to identified posterior cerebellar zones in rat (Suzuki et al. 2012). After injections in lobule VII they observed that most labeling occurred within the orbitofrontal and retrosplenial cortices and suggested a cerebellar impact on functions related to choice-making behavior (Mar et al. 2011) and performance in spatial learning tasks (St-Laurent et al. 2009), respectively. Indeed, such functions are in line with the autistic behaviors that were observed in patients affected by the Joubert's syndrome, an autosomal recessive disorder characterized by partial or complete agenesis of the cerebellar vermis (Holroyd et al. 1991), in GS Guinea pigs, a mutant strain that displays cerebellar abnormalities of lobule VII (Caston et al. 2003), and in rats subjected to early midline cerebellar lesion (Bobée et al. 2000).
These observations and the above mentioned alterations in the autistic posterior cerebellum observed at autopsy and/or sMRI converge to support the validity of the heterozygous *reln*$^{+/-}$ mouse to model human autism.

Animal models of autism-related synaptopathies: a comparison
Although autism is a multifactorial disease depending on both genetic and environmental factors for its development, evidence is accumulating that pathological synapses occur in the brain (Isshiki et al. 2014; Keller et al. 2017; Shinoda et al. 2013). Thus, it is worth noting that, postnatally, Reln appears to be able to modulate synaptic molecular composition and activity (see Lammert and Howell 2016). Indeed, several genes that have been associated with the autistic condition have been demonstrated to encode proteins that are directly or indirectly related with the synaptic structure and function. We will briefly discuss below the more relevant animal models related to these genes in the context of the present work.
PTEN encodes for a phospatidylinositol-3,4,5-trisphosphate3-phosphatase that negatively regulates the phosphatidylinositol-3-kinase (PI3K)/AKT signaling pathway, and *Pten* haplodeficient mice display behavioral changes like those observed in autistic patients (Clipperton-Allen and Page 2014). Additionally, conditional knockout mice in which *PTEN* inactivation was specifically induced in the Purkinje neurons also displayed behavioral autistic-like traits. Their mutant Purkinje neurons were hypertrophic with neuritic alterations and, consistently with our present findings, a degeneration of PF-PN synapses (Cupolillo et al. 2016).
SHANK3 encodes for a scaffolding protein in the postsynaptic density of glutamatergic synapses. The protein is important in synapse and dendritic spines development, learning and memory, and has been tightly associated with autism, after genomic studies (Monteiro and Feng 2017). *Shank3* deleted mice exhibit autistic behaviors and defects in striatal synapses and cortico-striatal circuits (Peça et al. 2011). A tightly linked gene, *IB2*, encodes for another protein of the postsynaptic density that, when disrupted in mice, reduces to about

45% the dendritic spread of the Purkinje neurons with a consequent reduction in thickness of the molecular layer, and induces motor and cognitive deficits like those in autism (Giza et al. 2010).

CNTNAP2 and CNTN6 have also been associated with autism. The former encodes for the CASPR2 protein, a transmembrane protein belonging to the neurexin superfamily, a group of cell-adhesion presynaptic proteins that intervene in synaptic plasticity *in vitro* (Anderson et al. 2012). The only two-photon study *in vivo* on mice lacking *CNTNAP2* showed that the Caspr2 stabilizes new synaptic circuitries in the somatosensory cortex (Gdalyahu et al. 2015), but a complete mapping of the CNS of these mice has not been published yet. There are no mice, at least to our knowledge, in which CNTN6 has been deleted, but deletion of CNTN1/F3 results in ataxia, with a derangement of the parallel fibers' orientation, reduction of the dendritic arbors of the granule cells and aberrant dendritic projections of the Golgi cells (Berglund et al. 1999). As CNTN1 is replaced by CNTN6 during normal cerebellar development (Stoeckli 2010) it would not be surprising that deletion of *CNTN6* gives rise to a similar phenotype.

SYNGAP1 encodes for the synaptic GTPase-activating protein 1 (SynGAP1), which is mutated in a minority of autism patients (Berryer et al. 2013). *Syngap* heterozygous (*Syngap*$^{+/-}$) mice show a range of behavioral, physiological, and anatomical abnormalities throughout development, among which an altered morphology of dendritic spines in CA1 pyramidal neurons (Barnes et al. 2015).

The SYN1 gene encodes for synapsin 1, a phosphoprotein belonging to the synapsin family, which is expressed at the cytoplasmic surface of the synaptic vesicles, has a key role in synaptogenesis and transmitter release regulation, and is mutated in some autistic families (Fassio et al. 2011). Notably, synapsin 1 knockout mice display autism-related behaviors (Greco et al. 2013), and, interestingly, a reduced phosphorylation of synapsin 1 is observed in the hippocampus of the Engrailed-2 (*EN-2*) knockout mice (Provenzano et al. 2015), another mouse model of autism (Kuemerle et al. 2007). *EN-2* is a homeobox gene that undergoes a complex epigenetic regulation in the autistic cerebellum where it was demonstrated that the Purkinje cell maturation, which normally follows the *EN-2* downregulation during development, can be impaired in some autistic patients (James et al. 2013).
Whereas all the gene products discussed so far intervene in shaping the cerebellar synapses and in the small synaptic vesicles' release machinery, the calcium-dependent activator protein for secretion 2 (CAPS2) regulates the release of dense-core vesicles, containing monoamines or neuropeptides (Merighi 2018) at both synaptic and non-synaptic sites. It is of interest to the present discussion that several copy number variations of *CAPS2* have been found in autistic patients (Shinoda et al. 2013). *Caps2* knockout mice display no obvious motor or sensory abnormalities, but, nonetheless, had cellular, morphological, physiological, and behavioral impairments (Shinoda et al. 2013). In lobules VI, VII, and XI delayed migration and increased cell death as well as reduced dendritic arborization of the Purkinje neurons were observed (Shinoda et al. 2013). Also, in the cerebral cortex and hippocampus the number of parvalbumin-positive interneurons was decreased at early postnatal stages (Shinoda et al. 2011).

Collectively, the structural and behavioral analysis of the above mouse models converges to demonstrate that synapses are a major target of several autism-related genes and proteins. However, the structural modifications that follow these mutations are often very subtle and difficult to be analyzed to prove or disprove a specificity of effects.

Conclusions

This study provides a quantitative description of the modifications in the expression of the presynaptic marker SYP1 and CNTN6 in the cerebellar vermis of *reln* haplodeficient mutant mice of both sexes. It demonstrates the existence of general (whole vermis) and specific (individual lobules) reductions in immunoreactivity that mainly, but not only, hit *reln*$^{+/-}$ male mice and are compatible with the view that these mice offer a useful model to study human autism. Our work is important to prompt further investigations on the structural changes of the cerebellar vermis of these mutants and, more generally, of the autistic cerebellum.

Table 1: Summary of quantitative analysis of the levels of expression of SYP1 and CNTN6 in the cerebellar vermis of Reeler mice of different genotypes

SYP1

Genotype	Vermis (whole)	ML	PL	GL	Vermian lobules										
					I	II	III	IV	V	VIa	VIb	VII	VIII	IX	X
reln$^{+/+}$♂															
reln$^{+/+}$♀															
reln$^{+/-}$♂															
reln$^{+/-}$♀															

Vermian lobules - molecular layer											
Genotype	I	II	III	IV	V	VIa	VIb	VII	VIII	IX	X
reln$^{+/+}$♂											
reln$^{+/+}$♀											
reln$^{+/-}$♂											
reln$^{+/-}$♀											

Vermian lobules - Purkinje cell layer											
Genotype	I	II	III	IV	V	VIa	VIb	VII	VIII	IX	X
reln$^{+/+}$♂											
reln$^{+/+}$♀											
reln$^{+/-}$♂											
reln$^{+/-}$♀											

Vermian lobules - granular layer											
Genotype	I	II	III	IV	V	VIa	VIb	VII	VIII	IX	X
reln$^{+/+}$♂											
reln$^{+/+}$♀											
reln$^{+/-}$♂											
reln$^{+/-}$♀											

CNTN6

Genotype	Vermis (whole)	ML	PL	GL
reln$^{+/+}$♂				
reln$^{+/+}$♀				
reln$^{+/-}$♂				
reln$^{+/-}$♀				

Summary of the most important differences in the level of expression of SYP1 among Reeler mice of different genotypes. Red cells filled indicate the occurrence of a statistically significant reduction in the expression of SYP1.

Abbreviations
BSA: Bovine serum albumin
CI: Confidence interval
CNTN6 = contactin 6
DAPI: 4′,6-diamidino-2-phenylindole
GL: Granular layer of the cerebellar cortex
HET: Heterozygous
IQ: Intelligence quotient
ML: Molecular layer of the cerebellar cortex
NGS: Normal goat serum
PFA: Percentage of the fluorescent area
PF-PN: Parallel fiber-to-Purkinje neuron
PL: Purkinje cells' layer of the cerebellar cortex
PPI: Pre-pulse inhibition
RELN: Reelin gene (human)
RELN: Reelin glycoprotein (human)
Reln: Reelin gene (mouse)
Reln: Reelin glycoprotein (mouse)
ROI: Region of interest
sMRI: Structural magnetic resonance imaging
SYP1: Synaptophysin 1
WT: Wild-type

Notes

Acknowledgements
The work described in this paper has been supported by local grants of the University of Turin. CC is in receipt of a grant of the Italian Ministry of Education and Research (MIUR)

Authors' contributions
CC collected animal samples, processed them for immunocytochemistry, acquired and processed IMF images, collaborated to statistical analysis and has been involved in drafting the manuscript and interpretation of data.
AM substantially contributed to the conception and design of the experiments, performed statistical analysis, interpreted data, and wrote the manuscript.
LL made substantial contributions to the conception and design of the study, collaborated to the acquisition of digital images and the interpretation of data, and critically revised the initial manuscript draft.

All authors agreed to be accountable for all aspects of the work in ensuring that questions related to the accuracy or integrity of any part of the work were appropriately investigated and resolved.

Compliance with ethical standard

The experiments described in this paper were carried out in accordance with the EU, Italian and institutional (Department of Veterinary Sciences) guidelines for the care and use of animals in scientific research.

Conflict of interest

The authors declare that they have no conflict of interest.

Ethical approval

The experiments described in this paper were approved by the Animal Welfare Committee of the Department of Veterinary Sciences of the University of Turin and by the Italian Ministry of Health (authorization n° 65/2016-PR).

Availability of data and material

The datasets generated and/or analyzed during the current study are available in the Online Resource OR.

Reference List

Abel JM, Witt DM, Rissman EF (2011) Sex differences in the cerebellum and frontal cortex: roles of estrogen receptor alpha and sex chromosome genes. Neuroendocrinol 93(4):230-40.

Ago Y, Condro MC, Tan YV, Ghiani CA, Colwell CS, Cushman JD, Fanselow MS, Hashimoto H, Waschek JA (2015) Reductions in synaptic proteins and selective alteration of prepulse inhibition in male C57BL/6 mice after postnatal administration of a VIP receptor (VIPR2) agonist. Psychopharmacol 232(12):2181-2189.

Andersen TE, Finsen B, Goffinet AM, Issinger OG, Boldyreff B (2002) A reeler mutant mouse with a new, spontaneous mutation in the reelin gene. Mol Brain Res 105(1-2):153-6.

Anderson GR, Galfin T, Xu W, Aoto J, Malenka RC, Südhof TC (2012) Candidate autism gene screen identifies critical role for cell-adhesion molecule CASPR2 in dendritic arborization and spine development. Proc Natl Acad Sci U S A 109(44): 18120-18125.

Azevedo Frederico AC, Carvalho Ludmila RB, Grinberg LT, Farfel JM, Ferretti Renata EL, Leite Renata EP, et al. (2009) Equal numbers of neuronal and nonneuronal cells make the human brain an isometrically scaled-up primate brain. J Comp Neurol 513(5):532-41.

Barnes SA, Wijetunge LS, Jackson AD, Katsanevaki D, Osterweil EK, Komiyama NH, Grant SG, Bear MF, Nägerl UV, Kind PC, Wyllie DJ (2015) Convergence of Hippocampal Pathophysiology in Syngap+/- and Fmr1-/y Mice. J Neurosci 35(45): 15073-15081.

Barr AM, Fish KN, Markou A, Honer WG (2008) Heterozygous reeler mice exhibit alterations in sensorimotor gating but not presynaptic proteins. Eur J Neurosci 27(10):2568-74.

Bauman ML (1991) Microscopic neuroanatomic abnormalities in autism. Pediatrics 87(5 Pt 2):791-6.

Bauman M, Kemper TL (1985) Histoanatomic observations of the brain in early infantile autism. Neurol 35(6):866-74.

Berglund EO, Murai K, Fredette B, Sekerkov, G, Marturano B, Weber L, Mugnaini E, Ranscht, B (1999). Ataxia and abnormal cerebellar microorganization in mice with ablated contactin gene expression. Neuron 24, 739–750.

Berryer MH, Hamdan FF, Klitten LL, Møller RS, Carmant L, Schwartzentruber J, Patry L, Dobrzeniecka S, Rochefort D, Neugnot-Cerioli M, Lacaille JC, Niu Z, Eng CM, Yang Y, Palardy S, Belhumeur C, Rouleau GA, Tommerup N, Immken L, Beauchamp MH, Patel GS, Majewski J, Tarnopolsky MA, Scheffzek K, Hjalgrim H, Michaud JL, Di Cristo G (2013) Mutations in SYNGAP1 cause intellectual disability, autism, and a specific form of epilepsy by inducing haploinsufficiency. Hum Mutat 34: 385–394.

Bey AL, Jiang YH (2014) Overview of mouse models of autism spectrum disorders. Curr Protoc Pharmacol 66:5-26.

Biamonte F, Assenza G, Marino R, D'Amelio M, Panteri R, Caruso D, et al. (2009) Interactions between neuroactive steroids and reelin haploinsufficiency in Purkinje cell survival. Neurobiol Dis 36(1):103-15.

Bobée S, Mariette E, Tremblay-Leveau H, Caston J. (2000) Effects of early midline cerebellar lesion on cognitive and emotional functions in the rat. Behav Brain Res 112(1):107-17.

Brigman JL, Padukiewicz KE, Sutherland ML, Rothblat LA (2006) Executive functions in the heterozygous reeler mouse model of schizophrenia. Behav Neurosci 120(4):984-8.

Brorson SH, Roos N, Skjorten F (1994) Antibody penetration into LR-White sections. Micron 25(5):453-60.

Burgoyne RD, Barclay JW (2002) Splitting the quantum: regulation of quantal release during vesicle fusion. Trends Neurosci 25(4):176-8.

Castagna C, Aimar P, Alasia S, Lossi L (2014) Post-natal development of the Reeler mouse cerebellum: An ultrastructural study. Ann Anat 196(4):224-35.

Castagna C, Merighi A, Lossi L (2016) Cell death and neurodegeneration in the postnatal development of cerebellar vermis in normal and Reeler mice. Ann Anat 207:76-90.

Caston J, Yon E, Mellier D, Godfrey HP, Delhaye-Bouchaud N, Mariani J (2003) An animal model of autism: behavioural studies in the GS guinea-pig. Eur J Neurosci 10(8):2677-84.

Catani M, Dell'acqua F, Thiebaut de Schotten M (2013) A revised limbic system model for memory, emotion and behaviour. Neurosci Biobehav Rev 37(8):1724-37.

Caviness VS, Rakic P (1978) Mechanisms of Cortical Development: A View From Mutations in Mice. Annu Rev Neurosci 1(1):297-326.

Clipperton-Allen AE, Page DT (2014). Pten haploinsufficient mice show broad brain overgrowth but selective impairments in autism-relevant behavioral tests. Hum Mol Genet 23: 3490–3505.

Codagnone MG, Podestá MF, Uccelli NA, Reinés A. (2015) Differential Local Connectivity and Neuroinflammation Profiles in the Medial Prefrontal Cortex and Hippocampus in the Valproic Acid Rat Model of Autism. Dev Neurosci 37(3):215-231.

Cousin MA, Evans G (2011) Activation of silent and weak synapses by cAMP-dependent protein kinase in cultured cerebellar granule neurons. J Physiol 589(Pt 8):1943-1955.

Courchesne E, Saitoh O, Yeung-Courchesne R, Press GA, Lincoln AJ, Haas RH, Schreibman L (1994) Abnormality of cerebellar vermian lobules VI and VII in patients with infantile autism: identification of hypoplastic and hyperplastic subgroups with MR imaging. AJR Am J Roentgenol. 162(1):123-30.

Courchesne E, Yeung-Courchesne R, Hesselink JR, Jernigan TL (1988) Hypoplasia of Cerebellar Vermal Lobules VI and VII in Autism. New Engl J Med 318(21):1349-54.

Cupolillo D, Hoxha E,, Faralli A, De Luca A, Rossi F, Tempia F, Carulli D (2016) Autistic-like traits and cerebellar dysfunction in Purkinje cell PTEN knock-out mice. Neuropsychopharmacol 41(6): 1457-1466.

D'Arcangelo G, Miao GG, Chen SC, Soares HD, Morgan JI, Curran T (1995) A protein related to extracellular matrix proteins deleted in the mouse mutant reeler. Nature 374(6524):719-23.

D'Arcangelo G, Miao GG, Curran T (1996) Detection of the reelin breakpoint in reeler mice. Brain Res Mol Brain Res 39(1-2):234-6.

Dean SL, McCarthy MM (2008) Steroids, sex and the cerebellar cortex: implications for human disease. Cerebellum 7(1):38-47.

D'Mello AM, Stoodley CJ (2015) Cerebro-cerebellar circuits in autism spectrum disorder. Front Neurosci 9:408.

D'Mello AM, Crocetti D, Mostofsky SH, Stoodley CJ (2015) Cerebellar gray matter and lobular volumes correlate with core autism symptoms. Neuroimage Clin 7:631-639.

DeSilva U, D'Arcangelo G, Braden VV, Chen J, Miao GG, Curran T, et al. (1997) The human reelin gene: isolation, sequencing and mapping on chromosome 7. Genome Res 7(2):157-64.

Ecker C, Spooren W, Murphy DG (2013) Translational approaches to the biology of Autism: false dawn or a new era? Mol Psychiatry 18(4):435-42.

Ekerot CF, Jörntell H (2001) Parallel fibre receptive fields of Purkinje cells and interneurons are climbing fibre-specific. Eur J Neurosci 13:1303-1310.

Ekerot CF, Jörntell H (2003) Parallel fibre receptive fields: a key to understanding cerebellar operation and learning. Cerebellum 2:101-109.

Falconer DS (1951) Two new mutants, 'trembler' and 'reeler', with neurological actions in the house mouse (*Mus musculus L.*). J Genet 50:192-201.

Falk J, Bonnon C, Girault J-A, Faivre-Sarrailh C (2002) F3/contactin, a neuronal cell adhesion molecule implicated in axogenesis and myelination. Biol Cell 94: 327–334.

Fassio A, Patry L, Congia S, Onofri F, Piton A, Gauthier J, Pozzi D, MessaM, Defranchi E, FaddaM, Corradi A, Baldelli P, Lapointe L, St-Onge J, Meloche C, Mottron I, Valtorta F, Nguyen D, Rouleau G, Benfenati F, Cossette P (2011) SYN1 loss-of-function mutations in autism and partial epilepsy cause impaired synaptic function. Hum Mol Genet 20(12):2297–2307.

Fatemi SH (2005) Reelin glycoprotein in autism and schizophrenia. Int Rev Neurobiol 71:179-87.

Fatemi SH, Aldinger KA, Ashwood P, Bauman ML, Blaha CD, Blatt GJ, et al. (2012) Consensus paper: pathological role of the cerebellum in autism. Cerebellum 11(3):777-807.

Fatemi SH, Stary JM, Halt AR, Realmuto GR (2001) Dysregulation of Reelin and Bcl-2 proteins in autistic cerebellum. J Autism Dev Disord 31(6):529-35.

Fykse EM, Takei K, Walch-Solimena C, Geppert M, Jahn R, De Camilli P, Südhof TC (1993) Relative properties and localizations of synaptic vesicle protein isoforms: the case of the synaptophysins. J Neurosci. 13(11):4997-5007.

Gdalyahu A, Lazaro M, Penagarikano O, Golshani P, Trachtenberg JT, Gescwind DH (2015) The autism related protein contactin-associated protein-like 2 (CNTNAP2) stabilizes new spines: an in vivo mouse study PLoS One, 10 Article e0125633.

Geyer MA (2008) Developing translational animal models for symptoms of schizophrenia or bipolar mania. Neurotox Res 14(1):71-8.

Giza J, Urbanski MJ, Prestori F, Bandyopadhyay B, Yam A, Friedrich V, Kelley K, D'Angelo E, Goldfarb M (2010) Behavioral and cerebellar transmission deficits in mice lacking the autism-linked gene islet brain-2. J Neurosci 30(44): 14805-14816

Goffinet AM (1984) Events governing organization of postmigratory neurons: Studies on brain development in normal and reeler mice. Brain Res Rev 7(3):261-96.

Greco B, Managò F, Tucci V, Kao HT, Valtorta F, Benfenati F (2013) Autism-related behavioral abnormalities in synapsin knockout mice. Behav Brain Res 251: 65-74.

Hadj-Sahraoui N, Frédéric F, Delhaye-Bouchaud N, Mariani J (1996) Gender Effect on Purkinje Cell Loss in the Cerebellum of the Heterozygous Reeler Mouse. J Neurogenet 11(1-2):45-58.

Halko MA, Farzan F, Eldaief MC, Schmahmann JD, Pascual-Leone A (2014) Intermittent Theta-Burst Stimulation of the Lateral Cerebellum Increases Functional Connectivity of the Default Network. J Neurosci 34(36):12049-56.

Halladay AK, Amaral D, Aschner M, Bolivar VJ, Bowman A, DiCicco-Bloom E, et al. (2009) Animal models of autism spectrum disorders: information for neurotoxicologists. NeuroToxicol 30(5):811-21.

Hansel C, Linden DJ, D'Angelo E (2001) Beyond parallel fiber LTD: the diversity of synaptic and non-synaptic plasticity in the cerebellum. Nature Neurosci 4 (5):467-75.

Herculano-Houzel S (2010) Coordinated Scaling of Cortical and Cerebellar Numbers of Neurons. Front Neuroanat. 10;4:12. https://doi.org/10.3389/fnana.2010.00012. eCollection 20104 ed.

Holroyd S, Reiss AL, Bryan RN (1991) Autistic features in Joubert syndrome: A genetic disorder with agenesis of the cerebellar vermis. Biol Psychiatry 29(3):287-94.

Hong SE, Shugart YY, Huang DT, Shahwan SA, Grant PE, Hourihane JO, et al. (2000) Autosomal recessive lissencephaly with cerebellar hypoplasia is associated with human RELN mutations. Nat Genet 26(1):93-6.

Hu J, Liao J, Sathanoori M, Kochmar S, Sebastian J, Yatsenko SA, Surti U (2015) CNTN6 copy number variations in 14 patients: a possible candidate gene for neurodevelopmental and neuropsychiatric disorders. J Neurodev Disord 7(1):26. https://doi.org/10.1186/s11689-015-9122-9.

Isshiki M, Tanaka S, Kuriu T, Tabuchi K, Takumi T, Okabe S (2014) Enhanced synapse remodelling as a common phenotype in mouse models of autism. Nat Commun. 5:4742. doi: 10.1038/ncomms5742.

James SJ, Shpyleva S, Melnyk S, Pavliv O, Pogribny IP (2013) Complex epigenetic regulation of engrailed-2 (EN-2) homeobox gene in the autism cerebellum. Transl Psychiatry 3:e232. doi: 10.1038/tp.2013.8.

Keller R, Basta R, Salerno L, Elia M (2017) Autism, epilepsy, and synaptopathies: a not rare association.Neurol Sci. 38(8):1353-1361.

Kemper TL, Bauman M (1998) Neuropathology of infantile autism. J Neuropathol Exp Neurol 57(7):645-52.

Kim KC, Choi CS, Gonzales ELT, Mabunga DFN, Lee SH, Jeon SJ, Hwangbo R, Hong M, Ryu JH, Han SH, Bahn GH, Shin CY (2017) Valproic Acid Induces Telomerase Reverse Transcriptase Expression during Cortical Development. Exp Neurobiol 26(5):252-265.

Krueger DD, Howell JL, Hebert BF, Olausson P, Taylor JR, Nairn AC (2006) Assessment of cognitive function in the heterozygous reeler mouse. Psychopharmacol (Berl) 189(1):95-104.

Kuemerle B, Gulden F, Cherosky N, Williams E, Herrup K (2007) The mouse Engrailed genes: a window into autism. Behav Brain Res 176(1): 121-132.

Lammert DB, Howell BW (2016) RELN Mutations in Autism Spectrum Disorder. Front Cell Neurosci 31 https://doi.org/10.3389/fncel.2016.00084

Limperopoulos C, Bassan H, Gauvreau K, Robertson RL Jr, Sullivan NR, Benson CB, et al. (2007) Does cerebellar injury in premature infants contribute to the high prevalence of long-term cognitive, learning, and behavioral disability in survivors? Pediatrics 120(3):584-93.

Magliaro C, Cocito C, Bagatella S, Merighi A, Ahluwalia A, Lossi L (2016) The number of Purkinje neurons and their topology in the cerebellar vermis of normal and reln haplodeficient mouse. Ann Anat 207:68-75.

Maloku E, Covelo IR, Hanbauer I, Guidotti A, Kadriu B, Hu Q, et al. (2010) Lower number of cerebellar Purkinje neurons in psychosis is associated with reduced reelin expression. Proc Natl Acad Sci USA 107(9):4407-11.

Mar AC, Walker ALJ, Theobald DE, Eagle DM, Robbins TW (2011) Dissociable Effects of Lesions to Orbitofrontal Cortex Subregions on Impulsive Choice in the Rat. J Neurosci 31(17):6398-404.

Mariani J, Crepel F, Mikoshiba K, Changeux JP, Sotelo C (1977) Anatomical, Physiological and Biochemical Studies of the Cerebellum from Reeler Mutant Mouse. Philos Trans R Soc Lond B Biol Sci 281(978):1-28.

Marrone MC, Marinelli S, Biamonte F, Keller F, Sgobio CA, Ammassari-Teule M, et al. (2006) Altered cortico-striatal synaptic plasticity and related behavioural impairments in reeler mice. Eur J Neurosci 24(7):2061-70.

Matsushita M, Okado N (1981) Spinocerebellar projections to lobules I and II of the anterior lobe in the cat, as studied by retrograde transport of horseradish peroxidase. J Comp Neurol 197(3):411-24.

McConnell SK (1995) Strategies for the generation of neuronal diversity in the developing central nervous system. J Neurosci 15(11):6987-98.

Mercati O, Huguet G, Danckaert A, André-Leroux G, Maruani A, Bellinzoni M, Rolland T, Gouder L, Mathieu A, Buratti J, Amsellem F, Benabou M, Van-Gils J, Beggiato A, Konyukh M, Bourgeois JP, Gazzellone MJ, Yuen RK, Walker S, Delépine M, Boland A, Régnault B, Francois M, Van Den Abbeele T, Mosca-Boidron AL, Faivre L, Shimoda Y, Watanabe K, Bonneau D, Rastam M, Leboyer M, Scherer SW, Gillberg C, Delorme R, Cloëz-Tayarani I, Bourgeron T (2017) CNTN6 mutations are risk factors for abnormal auditory sensory perception in autism spectrum disorders. Mol Psychiatry 22(4):625-633.

Mercer AA, Palarz KJ, Tabatadze N, Woolley CS, Raman IM (2016) Sex differences in cerebellar synaptic transmission and sex-specific responses to autism-linked Gabrb3 mutations in mice. Elife 5.

Merighi A (2018) Costorage of high molecular weight neurotransmitters in large dense core vesicles of mammalian neurons. Front Cell Neurosci 12:272. doi: 10.3389/fncel.2018.00272.

Michetti C, Romano E, Altabella L, Caruso A, Castelluccio P, Bedse G, et al. (2014) Mapping pathological phenotypes in reelin mutant mice. Front Pediatr 2:95. https://doi.org/10.3389/fped.2014.00095. eCollection@2014.

Miles JH (2011) Autism spectrum disorders--a genetics review. Genet Med 13(4):278-94.

Monteiro P, Feng G (2017) SHANK proteins: roles at the synapse and in autism spectrum disorder. Nat Rev Neurosci 18(3): 147-157

Morimura N, Yasuda H, Yamaguchi K, Katayama KI, Hatayama M, Tomioka NH, Odagawa M, Kamiya A, Iwayama Y, Maekawa M, Nakamura K, Matsuzaki H, Tsujii M, Yamada K, Yoshikawa T, Aruga J (2017) Autism-like behaviours and enhanced memory formation and synaptic plasticity in Lrfn2/SALM1-deficient mice. Nat Commun. 8:15800. doi: 10.1038/ncomms15800.

Murashima M, Hirano T (1999) Entire Course and Distinct Phases of Day-Lasting Depression of Miniature EPSC Amplitudes in Cultured Purkinje Neurons. J Neurosci 19(17):7326.

Navone F, Jahn R, Di Gioia G, Stukenbrok H, Greengard P, De Camilli P (1986) Protein p38: An integral membrane protein specific for small vesicles of neurons and neuroendocrine cells. J Cell Biol 103:2511-27.

Ognibene E, Adriani W, Granstrem O, Pieretti S, Laviola G (2007) Impulsivity–anxiety-related behavior and profiles of morphine-induced analgesia in heterozygous reeler mice. Brain Res 1131:173-80.

Oguro-Ando A, Zuko A, Kleijer KTE, Burbach JPH (2017) A current view on contactin-4, -5, and -6: Implications in neurodevelopmental disorders. Mol Cell Neurosci 81: 72-83.

O'Reilly JX, Beckmann CF, Tomassini V, Ramnani N, Johansen-Berg H (2010) Distinct and Overlapping Functional Zones in the Cerebellum Defined by Resting State Functional Connectivity. Cereb Cortex 20(4):953-65.

Peça J, Feliciano C, Ting G, Wang W, Wells M, Venkatramou T, Lascola C, Fu Z, Feng G (2011) Shank3 mutant mice display autistic-like behaviours and striatal dysfunction. Nature 472(7344): 437–442.

Podhorna J, Didriksen M (2004) The heterozygous reeler mouse: behavioural phenotype. Behav Brain Res 153(1):43-54.

Provenzano G, Pangrazzi L, Poli A, Sgadò P, Berardi N, Bozzi Y (2015) Reduced phosphorylation of synapsin I in the hippocampus of Engrailed-2 knockout mice, a model for autism spectrum disorders. Neurosci 286:122-130.

Robertson HR, Feng G (2011) Annual Research Review: Transgenic mouse models of childhood-onset psychiatric disorders. J Child Psychol Psychiatry 52(4):442-75.

Sakurai K, Toyoshima M, Ueda H, Matsubara K, Takeda Y, Karagogeos D, ShimodaY, Watanabe K (2009) Contribution of the neural cell recognition molecule NB-3 to synapse formation between parallel fibers and Purkinje cells in mouse. Dev Neurobiol 69(12):811-224.

Salinger WL, Ladrow P, Wheeler C (2003) Behavioral phenotype of the reeler mutant mouse: effects of RELN gene dosage and social isolation. Behav Neurosci 117(6):1257-75.

Schlerf JE, Galea JM, Spampinato D, Celnik PA (2015) Laterality Differences in Cerebellar-Motor Cortex Connectivity. Cereb Cortex 25(7):1827-34.

Schmahmann JD, Weilburg JB, Sherman JC (2007) The neuropsychiatry of the cerebellum - insights from the clinic. Cerebellum 6(3):254-67.

Schmitt U, Tanimoto N, Seeliger M, Schaeffel F, Leube RE (2009) Detection of behavioral alterations and learning deficits in mice lacking synaptophysin. Neurosci 162 (2): 234–43.

Schmitt A, Turck CW, Pilz PK, Malchow B, von WM, Falkai P, et al. (2013) Proteomic similarities between heterozygous reeler mice and schizophrenia. Biol Psychiatry 74(6):e5-e10.

Shinoda Y, Sadakata T, Furuichi T (2013) Animal models of autism spectrum disorder (ASD): a synaptic-level approach to autistic-like behavior in mice. Exp Anim 62(2): 71-78.

Shinoda Y, Sadakata T, Nakao K, Katoh-Semba R,Kinameri E, Furuya A, Yanagawa Y, Hirase H, Furuichi T (2011) Calcium-dependent activator protein for secretion 2 (CAPS2) promotes BDNF secretion and is critical for the development of GABAergic interneuron network. Proc Natl Acad Sci U.S.A. 108: 373–378.

Soiza-Reilly M (2015) Array Tomography: A Novel High-Resolution Immunofluorescence Technique. In: Immunocytochemistry and related techniques (Merighi A, Lossi L, Eds) Neuromethods 101: 377-388.

Stanfield AC, McIntosh AM, Spencer MD, Philip R, Gaur S, Lawrie SM (2008) Towards a neuroanatomy of autism: A systematic review and meta-analysis of structural magnetic resonance imaging studies. E Psychiatry 23(4):289-99.

Stoeckli ET (2010) Neural circuit formation in the cerebellum is controlled by cell adhesion molecules of the c ontactin family. Cell Adh Migr 4(4):523-526.

St-Laurent M, Petrides M, Sziklas V (2009) Does the cingulate cortex contribute to spatial conditional associative learning in the rat? Hippocampus 2009 19(7):612-22.

Stoodley CJ (2014) Distinct regions of the cerebellum show gray matter decreases in autism, ADHD, and developmental dyslexia. Front Syst Neurosci 8:92.

Stoodley CJ, Schmahmann JD (2010) Evidence for topographic organization in the cerebellum of motor control versus cognitive and affective processing. Cortex 46(7):831-44.

Sundberg M, Tochitsky I, Buchholz DE, Winden K, Kujala V, Kapur K, Cataltepe D, Turner D, Han MJ, Woolf CJ, Hatten ME, Sahin M5 (2018) Purkinje cells derived from TSC patients display hypoexcitability and synaptic deficits associated with reduced FMRP levels and reversed by rapamycin. Mol Psychiatry. 23(11):2167-2183.

Suzuki L, Coulon P, Sabel-Goedknegt EH, Ruigrok TJ (2012) Organization of cerebral projections to identified cerebellar zones in the posterior cerebellum of the rat. J Neurosci 2012 32(32):10854-69.

Tarsa L, Goda Y (2002) Synaptophysin regulates activity-dependent synapse formation in cultured hippocampal neurons. Proc Natl Acad Sci U S A. 99(2): 1012–1016.

Teixeira CM, Martín ED, Sahún I, Masachs N, Pujadas L, Corvelo A, et al. (2011) Overexpression of Reelin Prevents the Manifestation of Behavioral Phenotypes Related to Schizophrenia and Bipolar Disorder. Neuropsychopharmacol 36(12):2395-405.

Thiel G (1993) Synapsin I, Synapsin II, and Synaptophysin: Marker Proteins of Synaptic Vesicles. Brain Pathol 3(1):87-95.

Tissir F, Goffinet AM (2003) Reelin and brain development. Nat Rev Neurosci 4(6):496-505.

Tsai PT (2016) Autism and cerebellar dysfunction: Evidence from animal models. Semin Fet Neonat Med 21(5):349-55.

Tueting P, Costa E, Dwivedi Y, Guidotti A, Impagnatiello F, Manev R, et al. (1999) The phenotypic characteristics of heterozygous reeler mouse. Neuroreport 10(6):1329-34.

Ventruti A, Kazdoba TM, Niu S, D'Arcangelo G (2011) Reelin deficiency causes specific defects in the molecular composition of the synapses in the adult brain. Neurosci 189:32-42. https://doi.org/10.1016/j.neuroscience.2011.05.050. Epub@2011 Jun 2.

Voineagu I, Wang X, Johnston P, Lowe JK, Tian Y, Horvath S, Mill J, Cantor RM, Blencowe BJ, Geschwind DH (2011) Transcriptomic analysis of autistic brain reveals convergent molecular pathology. Nature 474(7351): 380-384.

White JJ, Sillitoe RV (2013) Development of the cerebellum: from gene expression patterns to circuit maps. Wiley Interdiscip Rev Dev Biol 2(1):149-64.

Wilson L, Sotelo C, Caviness VS Jr (1981) Heterologous synapses upon Purkinje cells in the cerebellum of the Reeler mutant mouse: an experimental light and electron microscopic study. Brain Res 213(1):63-82.